Doctoral Dissertation (Censored)

博士論文 （要約）

Study on Positional Signaling in Epidermis Differentiation in Arabidopsis thaliana.

(シロイヌナズナ表皮細胞分化における位置情報シグナルの分子的研究)

A Dissertation Submitted for the Degree of Doctor of Philosophy

December 2019

令和元年 12 月博士(理学)申請

Department of Biological Science, Graduate School of Science, The University of Tokyo

東京大学大学院理学系研究科生物科学専攻

Kenji Nagata

永田賢司

Table of contents

Abstract

Sessile lifestyle forces vascular land plants to endure a bewildering array of biotic and abiotic stresses. To survive in the hostile environments on land, plants are clad with the specialized defensive tissue called epidermis. Epidermis is a sheet-like tissue consisting of polarized epidermal cells that synthesize and secrete surface lipids to form a protective hydrophobic layer known as the cuticle. The strong adhesions between epidermal cells provides the first and most important line of defense against harmful invaders. Furthermore, the tight compression of inner cells by epidermal cells regulates and supports the growth and morphogenesis of the plant body that grows against gravity. Thus, epidermis forms a distinct cell layer covering the whole plant body, which is indispensable for a terrestrial lifestyle of plants.

However, regarding the process of the epidermis development, there is a long-standing debate of how cells know where they are. Because the protective and developmental regulatory function of the epidermis closely associates with their position within the body, the epidermis traits must be manifested by the cells located in the outermost cell location. To control such a spatial ordering of cell differentiation, positional signaling to transmit appropriate information on cell location is required, although the underlying molecular mechanism is largely unknown.

In my doctoral thesis, I tackled this issue by exploring the regulatory

mechanism of the epidermis-differentiation process with a special focus on the

ARABIDOPSIS THALIANA MERISTEM LAYER 1 (ATML1) protein, a master

regulator of protoderm/epidermis differentiation, and specialized lipid metabolism in the

epidermal cells. Firstly, I demonstrated that ATML1 is expressed in the outermost cells

with a distinct cell lineage. My detailed observation for ATML1 expression suggested

that such cell lineage- and position- dependence of ATML1 expression is attributed to

the autoregulatory mechanism for transcriptional activation of ATML1 and the protein

modification for post-transcriptional activation and/or inactivation of ATML1.

Secondly, I demonstrated that the introduction of W471L mutation into ATML1

disrupts the post-translational modification required for the function of ATML1. *In vitro*

protein-lipid binding assay revealed that W471L mutation specifically disrupts the

protein-lipid interaction between ATML1 and very-long-chain fatty acid-containing

ceramides (VLCFA-Cer). Consistently, very-long-chain fatty acid (VLCFA) depletion

from sphingolipid pool by specific inhibitor treatment caused the disruption of post-

translational modification of ATML1 and significantly decreases the transcription of

ATML1 likely via autoregulatory loop. Thus, the formation of ATML1-VLCFA-Cers

protein-lipid complex is indicated to be essential for the function of the ATML1 protein

and maintaining the autoregulatory expression of ATML1.

Lastly, I investigated the regulatory mechanism of VLCFA-Cers biosynthesis and localization. I found that PASTICCINO2 (PAS2), an essential enzyme for VLCFA biosynthesis, is expressed predominantly in the outermost cells. Furthermore, VLCFAs were significantly depleted from the sphingolipid pool in an epidermis-defective mutant. These results indicate that VLCFA-Cers biosynthesis is directly regulated by ATML1 and confined to outermost cells. In addition, VLCFA-Cers seem to be constituents of the apical membrane of outermost cells, and thus passed on to the outermost daughter cells after cell division.

These findings indicate that VLCFA-Cers may function as an essential molecular component that mediates the positional memory of outermost cells in epidermis differentiation. Collectively, I provide insights into a novel developmental strategy which evolved in plants.

Acknowledgment

First and foremost, I would like to express the deepest appreciation to Prof. Mitsutomo Abe for encouraging my Ph.D. study and for allowing me to grow as a professional scientist. He has been supportive since the days I started my research life as an undergraduate. Without his constructive feedback and continuous encouragement, I would not have been able to complete the dissertation. Moreover, his attitude to science has taught me by example what it means to be a good scientist.

I am deeply grateful to the members of my Ph. D committee, Prof. Ichiro Terashima, Prof. Hirokazu Tsukaya, Prof. Munetaka Sugiyama, Prof. Yuichiro Watanabe for guiding me through all these years. I also owe a very important debt to Prof. Hiroyuki Hirano for being part of my master thesis committee and continuous supports in my Ph.D. study. Prof. Ichiro Terashima, the chief examiner of my doctoral thesis, has been a wonderful role model for me since I decided to become a plant scientist. He has always been encouraging me and leading me in the right direction in every aspect of my life, sometimes over a glass of beer. Prof. Hirokazu Tsukaya let me know the importance of a sincere attitude toward scientific works, providing guidelines for me on the research life. Prof. Munetaka Sugiyama offered detailed and sophisticated advice, providing me a new perspective. Prof. Yuichiro Watanabe kindly accepted me since I

Abbreviations

3-AT	3-Amino-1,2,4-triazole
ACD	Asymmetric cell division
ACR4	ARABIDOPSIS CRINKLY4
ALE1	ABNORMAL LEAF SHAPE1
AP2	APETALA2
ATML1	ARABIDOPSIS THALIANA MERISTEM LAYER 1
AuxRE	Auxin responsive element
BASL	BREAKING OF ASYMMETRY IN THE STOMATAL LINEAGE
BiFC	Bimolecular fluorescent complementation
C1P	Ceramide-1-phosphatate
CDS	Coding sequence
DAG	Days after germination
DEK1	DEFECTIVE KERNEL 1
DMSO	Dimethyl sulfoxide
ECR	Enoyl-CoA reductase
EGFP	Enhanced green fluorescent protein
ER	Endoplasmic reticulum
FAE	Fatty acid elongase
FB1	Fumonisin B1
GSO1	GASSHO1
GSO2	GASSHO2
GIPC	Glycosyl inositol phospho ceramide
GL2	GLABRA2
GluCer	Glucosylceramide
GST	Glutathione S-transferase
H3K27me3	Trimethylated Lys residues at position 27 of histone H3
HCD	3-hydroxy acyl-CoA dehydratase
HD-ZIP	Homeodomain-leucine zipper
HSP	Heat-shock protein
hVLCFA	2-hydroxylated very-long-chain fatty acid
IPTG	Isopropyl β-D-1-thiogalactopyranoside
KCR	3-ketoacyl-CoA reductase
KCS	Ketoacyl-CoA synthase
LCB	Long-chain base

LCFA	Long-chain fatty acid
LOH1	LAG ONE HOMOLOGUE 1
LOH3	LAG ONE HOMOLOGUE 3
LR	Lateral root
LRP	Lateral root primordium
MAPK	Mitogen-activated protein kinase
MDCK	Madin-Darby canine kidney
MMC	Meristemoid mother cell
MS	Murashige and Skoog
NLS	Nuclear localization sequence
PAS2	PASTICCINO2
PCD	Programmed cell death
PCTP	Phosphatidylcholine transfer protein
PDF2	PROTODERMAL FACTOR2
PLO	Protein-lipid overlay
PR	Primary root
PS	Phosphatidylserine
REM1.2	Remorin 1.2
RT-PCR	Reverse transcription polymerase chain reaction
SLGC	Stomatal lineage ground cell
SM	Sphingomyelin
SMase	Sphingomyelinase
SPCH	SPEECHLESS
START	Steroidogenic acute regulatory protein (StAR)-related lipid-transfer
TF	Transcription factor
VLCFA	Very-long-chain fatty acid
VLCFA-Cers	Very-long-chain fatty acid-containing ceramides
WBC11	WHITE-BROWN COMPLEX HOMOLOG PROTEIN 11
YFP	Yellow fluorescent protein

Chapter-I

General Introduction

Functions of the epidermis in plant development

The differentiation of distinct cell types in appropriate patterns is a fundamental process

in the development of multicellular organisms (Scheres., 2001). In Arabidopsis,

epidermal cells differentiate as a single cell layer that covers the plant body. Because the

waxy cuticle layer of epidermal cells provides a protective barrier against hostile

terrestrial environments and the interlocking epidermal cells provide mechanical

strength, the arrangement of epidermal cells in the outermost cell layer is prerequisite

for successful terrestrial life. In addition, because the outermost cell position is suitable

for perceiving and responding to environmental changes, epidermal cells regulate plant

growth and morphology by integrating environmental and developmental signals

mediated by plant hormones and various signaling molecules (Galletti et al., 2016).

Thus, a successful terrestrial lifestyle necessitates the arrangement of epidermal cells at

the interface between a plant body and the environment.

Molecular mechanism involved in the differentiation of plant epidermal cells

Position-dependent differentiation of protoderm/epidermis requires the HD-ZIP

class IV family gene *ATML1* and its functionally redundant paralog *PROTODERMAL*

FACTOR2 (*PDF2*) (Lu et al., 1996; Abe et al., 2003; Ogawa et al., 2015). ATML1 and

PDF2 were previously shown to form homo- or hetero-dimers and specifically bind to the L1 box, an well-conserved *cis*-regulatory element within the promoter region of protodermal and epidermal cell-specific genes (Abe et al., 2001; Abe et al., 2003). Consequently, ATML1 and PDF2 can effectively orchestrate a variety of epidermis-specific events. Considering that the knock-out of both genes results in severe defects in shoot epidermal cell differentiation (Abe et al., 2003; Ogawa et al., 2015), ATML1 and PDF2 act as master regulators of epidermis differentiation. Consistent with their function, ATML1 and PDF2 are expressed exclusively in protodermal cells. Therefore, a transcriptional regulator which encode positional information for the surface position is required for the spatial regulation of these key genes.

Interestingly, an L1 box is also present in the promoter region of *ATML1* and *PDF2* (Abe et al., 2003). Furthermore, this L1-box-containing promoter region is sufficient for the epidermis-specific expression of the *ATML1* gene (Takada and Jurgens, 2007). These findings suggest an autoregulatory mechanism controlled by ATML1 and PDF2 directs the outermost cell-specific transcription of *ATML1* and *PDF2* (Abe et al., 2003). This autoregulatory loop appears to contribute to a stable inheritance of *ATML1* expression and epidermal-cell fate within clonal-epidermal cells that repeat anticlinal cell divisions (Schmidt, 1924).

During embryogenesis, however, inner cells diverge from outermost protodermal/epidermal cells (Goldberg et al., 1994; Jurgens, 1995). Early totipotent embryo, consisted of cells facing the external environment, stably express ATML1, indicating that they have protodermal-cell characteristics according to their location (Lu et al., 1996; Takada and Jurgens, 2007). Subsequently, inner cells diverge from these cells and build up a complicated inner structure. Thus, additional layers of regulation are required to prevent the inheritance of epidermal-cell fate in an inner-cell position.

Candidate genes and pathways involved in the radial positional signaling

To date, a series of molecular genetic studies have identified several candidate genes involved in epidermis differentiation. For example, an endosperm pathway, whose disruption results in arrested cuticle deposition on the cell surface during embryogenesis, is a candidate required for epidermis differentiation (Tanaka et al., 2001; Tsuwamoto et al., 2008; Yang et al., 2008; Xing et al., 2013). The endosperm pathway comprises the endosperm-specific transcription factor (TF) ZHOUPI (ZOU) (Yang et al., 2008), the subtilisin-like serine protease ABNORMAL LEAF SHAPE1 (ALE1) (Tanaka et al., 2001), and two paralogous receptor-like kinases GASSHO1(GSO1)/GASSHO2(GSO2) (Tsuwamoto et al., 2008) . The endosperm-

specific ZOU protein directs a variety of endosperm-specific gene expressions including

ALE1 (Yang et al., 2008). Because the subtilisin-like serine protease, which is encoded

by *ALE1*, is involved in the processing of peptide hormone precursors in animals

(Steiner, 1998), ALE1 is suggested to produce an endosperm-derived signal recognized

by GSO1/GSO2 in an embryo and activate the cuticle deposition in the embryo

(Tsuwamoto et al., 2008; Xing et al., 2013). Considering that the cuticle deposition on

the cell surface is a fundamental trait of the protodermal/epidermal cell, the

ZOU→ALE1→GSO1/GSO2 signaling relay mediates a putative signal that regulates the

epidermis differentiation process. *ARABIDOPSIS THALIANA HOMOLOGUE OF*

CRINKLY4 (ACR4) is also known as a candidate gene involved in the epidermis

differentiation process (Gifford et al., 2003; Watanabe et al., 2004). *ACR4* encodes a

receptor-like protein kinase localized to the basolateral membrane of epidermal cells

and its loss-of-function mutation results in various defects related to epidermal cell

differentiation including the impaired formation of the cuticle (Watanabe et al., 2004).

Interestingly, epidermal cell differentiation is affected synergistically by the

simultaneous loss of the *ACR4* and *ALE1* genes, suggesting ACR4 directs epidermis

differentiation independently of the endosperm pathway (Tanaka et al., 2007).

The lack of critical evidence for the direct involvement of these candidate

genes in the regulation of *ATML1* expression makes the situation complicated. Thus, in

this thesis, I revisit the question how the autoregulatory loop contributes to the spatial

regulation of *ATML1* expression.

Chapter-II

Materials and Methods

Materials and Methods

<u>Plant materials and growth conditions</u>

Columbia (Col) was used as wild-type Arabidopsis (*Arabidopsis thaliana*) in this study.

atml1-1 and *pdf2-1* and *atml1-3* have been described previously (Abe et al., 2003;

Ogawa et al., 2015). T-DNA insertion allele *pas2-3* (SALK_117051) was obtained from

the Salk Institute Genomic Analysis Laboratory T-DNA insertion lines

(http://signal.salk.edu). The primer sequence in genotyping assay are provided in Table

1. *gATML1-EGFP; atml1-3; pdf2-1* (#4), *gPAS2-EGFP; pas2-3* (#16), *HSP::NLS-*

mCherry; HSP::ATML1^{WT}-EGFP (#4) and *HSP::NLS-mCherry; HSP::ATML1^{W471L}-*

EGFP (#1) were generated in this study. *pAtREM1.2-YFP-AtREM1.2* transgenic plant

(Jarsch. et al., 2014) is kindly provided from T. Ott (Univ. of Freiburg) and M. Nagano

(Ritsumeikan Univ. Japan) and *proAtWBC11::GFP-AtWBC11* transgenic plant (Luo et

al., 2007) is kindly provided from X-Y. Chen (Chinese Academy of Sciences, China)

and H. Tanaka (Meiji Univ., Japan). Plants were grown on rock-wool bricks

supplemented with vermiculite or in petri dishes with Murashige and Skoog (MS) solid

medium supplemented with 1% (w/v) sucrose (Murashige and Skoog, 1962). Plants

were grown under long-day conditions (16 h light/8 h dark) under white fluorescent

light at 23°C.

<u>DNA constructs</u>

To generate the mutated ATML1 (ATML1^{W471L}), I amplified two truncated coding

sequence of ATML1 with W471L mutation (ATML1 W471L up and ATML1 W471L

down) by PCR. Primers for ATML1 W471L up were (F, 5'-

CACTGTTGATACATATGTATCATCCAAACATGTTC-3' and R, 5'-

AGCCACCAAACGTTTTGCACCGAAAGCTAA-3') and primers for ATML1 W471L

down were (F, 5'-AAACGTTTGGTGGCTACACTTGACCGCCAA-3' and R, 5'-

ATTCAGAATTGTCGAGGCTCCGTCGCAGGCCAGAGC-3'). The purified PCR

products were cloned together into NdeI and SalI sites of pRI201AN vector (TaKaRa)

using In-Fusion® HD Cloning Kit (TaKaRa) to generate pRI201AN_ATML1^{W471L}.

pRI201AN_ATML1^{W471L} was used as the PCR template for plasmid constructions in

this study.

To construct vectors for heat pulse induction assay, I amplified the promoter

region of HSP18.2 by PCR using primers as follows: (F, 5'-

CCAAGCTTGCATGCCAAGCTTTTCTCTTCATTTCTC-3' and R, 5'-

TGTTCGTTGCTTTTCGGGAGA-3'). Next, the protein coding sequence of NLS-

17

mCherry, ATML1^{WT}, ATML1^{W471L} and EGFP were amplified using appropriate

templates by PCR. Primers for NLS-mCherry were (F, 5'-

GAAAAGCAACGAACACATATGCGACCCCCAAAGAAGAAG-3' and R, 5'-

ATTCAGAATTGTCGATTACTTGTACAGCTCGTCCAT-3'), primers for ATML1^{WT}

and ATML1^{W471L} were (F, 5'-

GAAAAGCAACGAACACATATGTATCATCCAAACATGTT-3' and R, 5'-

ACTAGTGGCTCCGTCGCAGGCCAGAGC-3'), and primers for EGFP were (F, 5'-

GACGGAGCCACTAGTATGGTGAGCAAGGGCGAGGAG-3' and R, 5'-

ATTCAGAATTGTCGATTACTTGTACAGCTCGTCCAT-3'). Subsequently, the PCR-

amplified HSP promoter and NLS-mCherry were cloned together into PstI and SalI sites

of pRI201AN vector using In-Fusion® HD Cloning Kit to generate

pRI201AN_HSP::NLS-mCherry::HSP ter. The PCR-amplified HSP promoter, ATML1

^{WT} and EGFP fragments were cloned together into PstI and SalI sites of pRI201AN

vector using In-Fusion® HD Cloning Kit to generate pRI201AN_HSP::ATML1^{WT} -

EGFP::HSP ter. The PCR-amplified HSP promoter, ATML1^{W471L}, and EGFP fragments

were cloned together into PstI and SalI sites of pRI201AN vector using In-Fusion® HD

Cloning Kit to generate pRI201AN_HSP::ATML1^{W471L}-EGFP::HSP ter. Finally, the

sequence of HSP::ATML1 ^{WT} -EGFP::HSP ter and HSP::ATML1^{W471L}-EGFP::HSP ter

was amplified by PCR using primers as follows: (F, 5'-

CGGCCGCTGGATCCCAAGCTTTTCTCTTCATTTCTC-3' and R, 5'-

TGATTACGAATTCCCCTTATCTTTAATCATATTCCA-3'). The purified

HSP::ATML1^{WT}-EGFP::HSP ter and HSP::ATML1^{W471L}-EGFP::HSP ter PCR products

were cloned into SmaI site of HSP::NLS-mCherry::HSP ter using In-Fusion® HD

Cloning Kit to generate pRI201AN_HSP::NLS-mCherry::HSP ter; HSP::ATML1^{WT}-

EGFP::HSP ter and pRI201AN_HSP::NLS-mCherry::HSP ter; HSP::ATML1^{W471L}-

EGFP::HSP ter, respectively.

To construct gATML1-EGFP, I generated the DNA fragments containing

BamHI and EcoRI restriction sites between loxP site by annealing of following primers

after denaturing: (F, 5'-CACCATAACTTCGTATAGCATACATTATAC

GAAGTTATGGATCCCGAATTCATAACTTCGTATAGCATACATTATACGAAGTTA

T-3' and R, 5'-

ATAACTTCGTATAATGTATGCTATACGAAGTTATGAATTCGGGATCCATABRAC

TTCGTATAATGTATGCTATACGAAGTTATGGTG-3'). Subsequently, this DNA

fragments were inserted into pENTR™/D-TOPO® Vector according to the

manufacturer's instructions to generate pENTR/D_loxP_BamHI-EcoRI_loxP. Then, the

sequence of EGFP and 3' UTR sequence of ATML1 were amplified by PCR (EGFP and

ATML1 ter, respectively). Primers for EGFP were (F, 5'-

TTATGGATCCCGAATTCGTGAGCAAGGGCGAGGAGCTGTT-3' and R, 5'-

AAACATCGATTACTTGTACAGCTCGTCCAT-3') and primers for ATML1 ter were

(F, 5'-CAAGTAATCGATGTTTTCGGGTAAGCTTTTTT-3' and R, 5'-

TACGAAGTTATGAATTTGATGACTTGGTCTCCATAATTTC-3'). The purified

EGFP PCR products and ATML1 ter PCR products were cloned together into EcoRI

sites of pENTR/D_loxP_BamHI-EcoRI_loxP vector using In-Fusion® HD Cloning Kit

to generate pENTR/D_loxP_BamHI-EcoRI-EGFP-ATML1 ter-loxP. Next, promoter and

protein coding sequence of ATML1 were amplified by PCR using primers as follows:

(F, 5'-ACGAAGTTATGGATCCAAGCTTAGTTTCTTATTTGACATA -3' and R, 5'-

CCTTGCTCACGAATTCGGCTCCGTCGCAGGCCAGAGC-3'). The purified

promoter and protein coding sequence of ATML1 PCR products were cloned into

BamHI and EcoRI sites of pENTR/D_loxP_BamHI-EcoRI-EGFP-ATML1 ter-loxP

using In-Fusion® HD Cloning Kit to generate pENTR/D_loxP-gATML1-EGFP-loxP.

pENTR/D_loxP-gATML1-EGFP-loxP was subsequently recombined into the binary

expression vector (pHGW.0) using Gateway LR Clonase II enzyme mix (Thermo Fisher

Scientific) and pHGW_loxP-gATML1-EGFP-loxP was generated.

To construct gPAS2-EGFP, I amplified the sequence of EGFP between loxP

sites by PCR using primers as follows: (F, 5'-CCAAGCTTGCATGCCATA

ACTTCGTATAGCATACATTATACGAAGTTATGGATCCGGTGGTGGTGGTGGTG

TCGAC-3' and R, 5'-

CCATGATTACGAATTATAACTTCGTATAATGTATGCTATACGAAGTTATGAATTC

TTACTTGTACAGCTCGTCCAT-3'). The purified loxP-EGFP-loxP PCR products was

cloned into PstI and EcoRI sites of pRI201AN vector using In-Fusion® HD Cloning Kit

to generate pRI201AN_loxP-EGFP-loxP. Next, 3'UTR sequence of PAS2 (PAS2 ter)

was amplified by PCR using primers as follows: (F, 5'-

GTACAAGTAAGAATTAAGAAAAGATTTAGAAAGAGACGAA-3' and R, 5'-

ACGAAGTTATGAATTCAATTTCATAAATATTATTAAGAATCC-3'). The purified

PAS2 ter PCR products were cloned into EcoRI site of pRI201AN_loxP-EGFP-loxP

using In-Fusion® HD Cloning Kit to generate pRI201AN_loxP-EGFP-PAS2 ter-loxP

Finally, promoter and protein coding sequence of PAS2 (PAS2 up) were amplified by

PCR using primers as follows: (F, 5'-

ACGAAGTTATGGATCCGGAATATCCACTGTTAGCTT-3' and R, 5'-

CACCACCACCGGATCCTTCCCTCTTGGATTTGGAGAG-3'). The PCR-amplified

PAS2 up PCR products were cloned into BamHI site of pRI201AN_loxP-EGFP-PAS2

ter-loxP using In-Fusion® HD Cloning Kit to generate pRI201AN_loxP-gPAS2-EGFP-

loxP.

該当部分に関して、5 年以内に雑誌で刊行予定のため、非公開。

該当部分に関して、5 年以内に雑誌で刊行予定のため、非公開。

To construct vectors for protein expression, I amplified the coding sequences of START domain of ATML1 and ATML1^{W471L} by PCR using primers as follows: (F, 5'-AGGGCCCGGGACATATGATACCTTCTGAGGCTGATAAG-3' and R, 5'-AGATTACCTATCTAGAACAAGCCGGAATGTTGCTGGC-3'). The PCR-amplified START and START^{W471L} fragments were cloned into NdeI and XbaI sites of pCold™_GST DNA (TaKaRa) using In-Fusion® HD Cloning Kit to generate pCOLD_GST-START and pCOLD_GST-START^{W471L}, respectively.

24

該当部分に関して、5 年以内に雑誌で刊行予定のため、非公開。

該当部分に関して、5 年以内に雑誌で刊行予定のため、非公開。

Transformation of Arabidopsis

The constructs described above in binary vectors were introduced into *Agrobacterium tumefaciens* strain GV3101 and transformed into Arabidopsis plants by the floral-dip procedure (Clough and Bent, 1998).

Agroinfiltration of Nicotiana benthamiana leaf epidermal cells and BiFC analysis

Agroinfiltration of *Nicotiana benthamiana* leaf epidermal cells and subsequent BiFC analysis were performed as described previously (Terakura et al., 2007).

Microscopy

Confocal microscopy was performed using an LSM 510 Meta Confocal laser-scannning microscope (Carl Zeiss) or a C2 confocal Microscope (Nikon). For observation of the fluorescence signal during embryogenesis, the embryos were excised from the ovules in 20% (v/v) glycerol solution.

Heat pulse treatment and RT-PCR analysis

For heat pulse induction of HSP18.2 promoter activity, whole plants were submerged into 1/2 MS liquid medium and incubated in a water bath for 3 hours at 35°C. For RT-PCR analysis, total RNA was extracted from frozen tissues by using TRIzol reagent

(Thermo Fisher Scientific) and was treated with RNase-free DNase (Thermo Fisher

Scientific) according to the manufacturer's instructions. Total RNA (1 μg) was reverse-

transcribed with an oligo dT primer according to the protocols of the Superscript II

(Thermo Fisher Scientific). The primer sequence and PCR conditions are provided in

Table 2.

Drug treatment

Both Fumonisin B1 (FB1; Sigma-Aldrich) and cafenstrol (FUJIFILM Wako Pure

Chemical Corporation) were dissolved in dimethyl sulfoxide (DMSO) and added to

media so that the solvent concentration did not exceed 0.1% (v/v). For long-term

treatment, seedlings were directly germinated on MS solid media supplemented with 0.5

μM Fumonisin B1 or 0.3 μM cafenstrol. For Fumonisin B1 short-term treatment, 7 days

after germination (7DAG) seedlings were transferred to 1/2 MS liquid media

supplemented with 3 μM FB1 and incubated for 24 hours. In each experiment, mock

treatment (0.1% (v/v) DMSO treatment) was performed as a control experiment.

Real-time RT-PCR analysis

Total RNA was extracted from frozen 5DAG seedlings by using TRIzol reagent (Thermo Fisher Scientific) and was treated with RNase-free DNase (Thermo Fisher Scientific) according to the manufacturer's instructions. Total RNA (1 μg) was reverse-transcribed with an oligo dT primer according to the protocols of the Superscript II (Thermo Fisher Scientific). The resulting cDNA diluted 1:4 in nuclease-free water and 1 μl aliquots were analyzed. Real-time RT-PCR was carried out using a Light Cycler® 480II (Roche). Reactions were run in triplicate in two experimental replicates at least. The mean of housekeeping gene *PP2A* (*PROTEIN PHOSPHATASE 2A SUBUNIT A3*) was used as an internal control to normalize the variability in expression levels. The primer sequence and probe list (Light Cycler® 480 Probe Master (Roche)) are provided in Table 3.

<u>Lipid analysis</u>

Sphingolipid contents in lyophilized Arabidopsis tissues were determined using LC-MS/MS with a targeted monitoring method as described previously (Ishikawa et al., 2018).

該当部分に関して、5 年以内に雑誌で刊行予定のため、非公開。

29

該当部分に関して、5 年以内に雑誌で刊行予定のため、非公開。

Protein-lipid interaction analysis

RossettaII (Novagen) cultures expressing pCOLD_GST-START or pCOLD_GST-

STARTW471L constructs were grown in 200 mL LB (Luria-Bertani) liquid medium till

an OD600 of 0.4-0.6, and then transferred to an ice-cold water bath for 10 min. After 10

min incubation in the ice-cold water bath, cell cultures were incubated at 15°C for 30 min, and then the expression of GST tagged recombinant proteins was induced by 1 mM isopropyl-thiogalactoside (IPTG). After induction, cells were cultivated at 200 rpm for 24 h at 15°C. Subsequently, the cells were harvested by centrifugation at 10,000 g for 10 min at 4°C. The cell-pellet was re-suspended in 10 mL of Bugbuster master mix, and the cell suspension was rotated gently at room temperature for 10 min. The cell suspension was centrifuged at 16,000 g for 20 min at 4°C and the supernatant which contained soluble GST tagged recombinant proteins was collected. GST-tagged recombinant proteins were purified by using glutathione sepharose 4B according to the manufacturer's instructions.

To enable investigations of sphingolipids-protein interactions, I originally prepared sphingolipids-spotted membrane. C16 Ceramide (d18:1/16:0), C24 Ceramide (d18:1/24:0), C16 Ceramide-1-Phosphate (d18:1/16:0) and C24 Ceramide-1-Phosphate (d18:1/24:0) were purchased from Avanti Polar Lipids (USA). Glucosylceramide from Rice (Glucosylceramide mix.) was purchased from Nagara science (JAPAN). These lipids were dissolved in Methanol/chloroform (1:1) to a concentration of 100 μM. GIPC fractions were prepared from Arabidopsis shoots by the method with isopropanol/hexane/water extraction, followed by fractionation with weakly-anion

exchange chromatography as in Ishikawa et al. (2016). Purity of the GIPC fraction was

determined by LC-MS/MS, in which no other sphingolipid classes were detected. The

fraction was finally dissolved in 2-propanol/water/hexane (55:20:5) to a concentration

of 100 μM. Two μL aliquots of each lipid solution were directly spotted onto

nitrocellulose membrane (Amersham Protran Supported 0.45 μm). For investigation of

lipid-protein interaction other than those above, Sphingo Strips and PIP Strips were

obtained from Echelon Biosciences. The lipid overlay assay was performed according to

Dowler et al. (2002). The membranes were blocked for 1 h at room temperature in

blocking buffer (2 mg/mL fatty-acid-free BSA, 150 mM NaCl, 50 mM Tris-HCl pH 7.5,

0.1% (v/v) Tween 20). The membranes were then incubated for 2 h at room temperature

in the presence of 1μg/mL purified GST tagged recombinant proteins. The membranes

were probed with a polyclonal anti-GST antibody (MBL; 1:1000 in blocking buffer) for

1h at room temperature. The secondary antibody, Anti-Rabbit IgG, HRP-Linked Whole

Ab Donkey (GE Healthcare; 1:5000 in TBST), was incubated with the membrane for 1h

at room temperature. Bound antibody was visualized with the Ez West Lumi One

(ATTO). The signals were collected using an Image Quant LAS 4000 mini (GE

Healthcare Japan). The mean of signal intensity was measured by using Image J

software.

Table. 1 The primer sequence for genotyping assay.

Primer name	Forward primer (5'→3')	Reverse primer (5'→3')	Target sequence
P1 and P2	TCCAAAAATTGATAGGCATC	ATAAAGAAAAAAGCTTACCCG	*ATML1*
P3 and P4	GATCAGTGCCTTGAAGGAAA	CTGTTGTCGACATTGTTGTC	*PDF2*
P5 and P6	TGTTGTCCTTCCTACAGAAGC	AGCCTTGAACCTATCTGTGGC	*PAS2*
P7 and P8	AGGCGAGTGGTTCTTTGTTTT	TCACTCAACAACATCGAGCAC	*FLC*

Table. 2 The primer sequence and PCR conditions for RT-PCR analysis.

Gene	Forward primer (5'→3')	Reverse primer (5'→3')	annealing temp.	cycles
ATML1 $^{WT/W471L}$ -EGFP	TGGATGATCCGGGAAGACCT	CTCGCCCTTGCTCACCATAC	50	30
NLS-mCherry	GACCCCCAAAGAAGAAGCGTA	CTGCTTGATCTCGCCCTTCA	50	30
TUBULIN BETA CHAIN 2	CTCAAGAGGTTCTCAGCAGTA	TCACCTTCTTCATCCGCAGTT	50	30

Table. 3 The primer sequence and probe list for qRT-PCR analysis.

Gene	Forward primer (5'→3')	Reverse primer (5'→3')	Probe
ATML1	GGAATAGTGTCTCCTTGCTTCG	TGATGCGTCCGTACAACTTT	122
PDF2	TCTCCTTGCTCCGAGTCAATA	TGCATCTGTACAGCTCTCTTGTAGA	106
PP2A	ATTCCGATAGTCGACCAAGC	AACATCAACATCTGGGTCTTCA	22

Chapter-III

Analysis of influence of cell position and cell lineage on ATML1 expression

Introduction

The differentiation of epidermis, a fundamental plant tissue located in the interface

between a plant body and environment, requires a robust system that mediates the

positional information of cell location. Although the extensive identifications of genes

related to epidermis differentiation as described in chapter-I, a deterministic regulatory

mechanism that regulates the expression of *ATML1* and *PDF2* remains unclear.

Therefore, in chapter-II, I first attempted to gain a precise understanding of the

transcriptional logic governing the expression of *ATML1* through detailed observations

of the spatial expression patterns of *ATML1*.

In plants, the importance of cell position, rather than cell lineage, in

determining cell fate is widely recognized (Stewart and Dermen, 1975; van den Berg et

al., 1995; Scheres, 2001; Leyser and Day, 2009). For example, histological analysis has

previously shown that inner cells of plants, which derive from occasional periclinal

divisions of outermost cells, develop according to their positions rather than their

outermost cell lineage (Stewart and Dermen, 1975). Thus, models for the epidermal cell

differentiation, emphasizing the importance of their cell location, have been proposed as

well as the models for the differentiation of other cell types. In contrast, the ablation of

tissues does not result in *de novo* acquisition of epidermal identity in the surface

position (Bruck and Walker, 1985), indicating the existence of non-epidermal cells

located in an outermost position in contradiction to the conventional model.

I, therefore, reexamine the validity of the conventional view of plant cell

differentiation by a detailed expression analysis of ATML1 as a molecular determinant

of the epidermal cell fate. However, it is difficult to dissociate the effect of cell lineage

to *ATML1* expression from that of cell position in the protodermal/epidermal cells of

embryos and shoots in which intensive investigations of ATML1 expression has been

already carried out. Specification of protodermal cells, or incipient epidermal cells, take

place in the 16-cell (dermatogen) stage embryo and represents the first manifestation of

radial axis polarity (Goldberg et al., 1994; Jurgens, 1995). Because of the epidermal cell

traits that undergo predominantly anticlinal divisions (Schmidt, 1924), the protodermal

cells at the dermatogen stage become the common ancestral cells of all

protodermal/epidermal cells of the embryos and the shoots. Thus, protoderm/epidermal

cells of the embryos and the shoots have an identical cell lineage (Fig. II-1a, b).

In contrast, the developmental ontogeny of outermost cells of roots is distinct

from that of the embryonic and aerial epidermal cells (Fig. II-1c, d). Previous analyses

using histological techniques and clonal analysis revealed that the outermost lineage of

embryos is maintained in the initial outermost root cap cells of primary roots (PRs) ,

although the epidermal cells of elongated PRs are originated from an inner cell lineage

of embryos (Scheres et al., 1994). Furthermore, outermost-lineage cells are shed from

PRs though the first root-cap detachment, and thus an outermost cell position is

occupied by inner lineage cells in mature PRs (Kumpf and Nowack, 2015). Thus, root is

a suitable system for dissociating the effect of cell lineage to ATML1 expression from

the effect of cell position.

My detailed expression analysis provides strong evidence that outermost cell

position alone is not sufficient for epidermis differentiation and that outermost lineage is

also involved in this process, revealing the novel regulation layer of cell fate

determination in plants.

Results

Influence of cell lineage on *ATML1* expression

I generated transgenic Arabidopsis harboring a *gATML1-EGFP* construct that can rescue *atml1-3; pdf2-1* from lethality (Fig. II-2a-d). Consistent with previous *in situ* hybridization and promoter analyses (Lu et al., 1996; Sessions et al., 1999; Takada and Jurgens, 2007), epidermal-cell specific expression pattern of ATML1-EGFP was observed in embryos and above-ground tissue (Fig. II-2e-i). To understand the role of cell lineage in the expression of *ATML1*, I analyzed the expression pattern of ATML1-EGFP in root cells located in the equivalent position but derived from distinct cell lineages. Intriguingly, ATML1-EGFP was detected in the initial outermost root cap cells in PRs just after germination, although not in epidermal cells (Fig. II-3a, b, d). Furthermore, I could no longer observe EGFP fluorescence in the outermost cells in PRs after root-cap detachment (Fig. II-3c, e).

These observations were further supported by the observation of EGFP in lateral roots (LRs) of *gATML1-EGFP; atml1-3; pdf2-1*(Fig. II-4). The divergence of outermost lineage and inner lineage firstly takes place at the stage-II LR primordium (LRP) during the LR development (Malamy and Benfey, 1997). The outermost lineage cells at this stage subsequently divide and give rise to the epidermal cells and outermost

40

root cap cells of young LRs (Malamy and Benfey, 1997). In addition, as well as PRs,

through the detachment of root cap cells, outermost-lineage cells are shed from LRs

(Fig. II-4f). In contrast to the observations in PRs, the expression of ATML1-EGFP was

maintained in both the epidermis and outermost root cap cells of LRPs and young LRs

(Fig. II-4a, b, d, e), but not in outermost cells after the detachment of root cap cells (Fig.

II-4c, f).

Collectively, these observations strongly suggest that the expression of ATML1

is dependent on outermost lineage and that the outermost-cell position alone is not

sufficient for its expression.

Influence of cell position on *ATML1* expression

To investigate how the expression of *ATML1* necessitates the outermost cell position, I

examined the expression pattern of ATML1-EGFP in cells located in a distinct position

but derived from a common mother cell. For this purpose, I carefully observed the

dermatogen stage of *gATML1-EGFP* embryos, whose outermost cells and inner cells are

derived from common outermost cells of 8-cells (octant) stage embryos (Goldberg et al.,

1994; Jurgens, 1995). In the majority of the 16-cell-stage embryos, ATML1-EGFP

fluorescence was limited to the outermost cells (Fig. II-5c, f). However, EGFP

41

fluorescence was sometimes also observed in the inner cells probably because ATML1-

EGFP can be passed on to the inner cells though the periclinal-asymmetric division

(Fig. II-5a, b, d, e). These observations suggest that the outermost cell position is

required for the expression of *ATML1* and that the inability of inner cells to differentiate

into the epidermis is not due to asymmetric segregation of ATML1 protein.

Cell lineage- and cell position-dependent post-translational regulation of ATML1

A previous promoter assay revealed that the transcription from the *ATML1* promoter in

the inner cells is strictly repressed immediately after periclinal-asymmetric division to

the dermatogen stage (Takada and Jurgens, 2007). This previous analysis in cooperation

with the EGFP fluorescence in inner cells of the dermatogen stage suggests that ATML1

in the inner cells may be unable to activate the positive feedback.

To assess this hypothesis, I used a heat-inducible transient-expression system of

ATML1^{WT}-EGFP and *NLS-mCherry* in LR cells (Fig. II-6) (Takahashi et al., 1992). RT-

PCR analysis confirmed that the transcriptions of both transgenes can be induced in the

transgenic Arabidopsis by a single pulse of heat treatment (Fig. II-7). In young LRs, the

fluorescence of mCherry, which was monitored as a heat-pulse induction control, was

observed in all cells after heat treatment (Fig. II-8). By contrast, EGFP fluorescence was

observed in the nuclei of the outermost cells but not in those of the inner cells, reflecting

the endogenous pattern of ATML1 expression (Fig. II-8). Moreover, ATML1^{WT}-EGFP

fluorescence was not observed even in the outermost cells of LRs after the detachment

of root cap cells (Fig. II-9). These observations indicate that the functional property of

the ATML1 protein is modified according to cell position.

Discussion

In this chapter, I first showed that, even though the cells occupy the outermost cell position, they cannot stably express ATML1 protein because they have an inner cell lineage (Fig. II-3, 4, 9). This result demonstrates the requirement for the specific cell lineage in the expression of *ATML1*. Autoregulatory loop, which regulates the expression of *ATML1* and *PDF2*, provides robustness of gene expression within a clonal lineage, although it cannot induce *de novo* gene expression. Thus, I concluded that the inheritance of an autoregulatory loop within a clonal lineage plays a pivotal role in the regulation of ATML1 expression.

I also found that *ATML1* expression is inherited to both daughter cells through a periclinal-asymmetric division of outermost cells but attenuated only in the inner daughter cell (Fig. II-5). This result suggests that an unrevealing mechanism prevents the inheritance of the autoregulatory loop in an inner-cell position by altering the functional property of the ATML1 protein. Moreover, based on the observations of ATML1 protein after a transient and ectopic induction (Fig. II-8, 9), I propose that the stability of ATML1 protein is regulated in a position-dependent manner and this hypothesis might explain the observed position-dependent functional modulation of ATML1 protein.

Collectively, these results are compatible with practical experience and observation which support the importance of cell position or cell lineage for *ATML1* expression rather than conventional theories, confirming these observations are beneficial for understanding the principles of the regulation of *ATML1* expression.
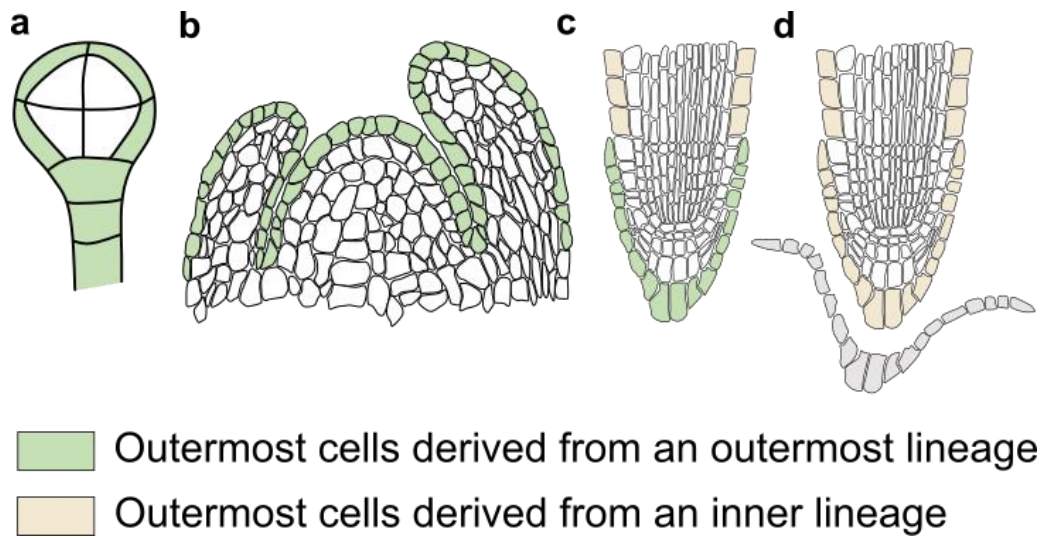
Fig. II-1 Cell lineage distribution atlas of the plant body

a-d, Schematics representation of outermost lineage distribution at various

developmental stages and tissues. **(a),** Dermatogen stage embryo. **(b),** Shoot apical

meristem and leaf primordia. **(c),** Primary root before root-cap detachment. **(d),** Primary

root after root-cap detachment. In this study, Root cells are classified as outermost cells

derived from an outermost lineage (green), outermost cells derived from an inner

lineage (pale orange), or inner cells (white).

a

WT   *gATML1-EGFP*   *gPAS2-EGFP*
            ;atml1-3;pdf2-1   *;pas2-3*

b

atml1-3   *atml1-1*   500bp

ATML1

pdf2-1

PDF2

c

transgene   promoter+coding sequence   EGFP/EYFP   terminator

P1   P2

atml1-3

P3   P4

pdf2-1

d

P1+P2   P3+P4   P5+P6 (*FLC*)

e   **f**   **i**

g   **h**

47
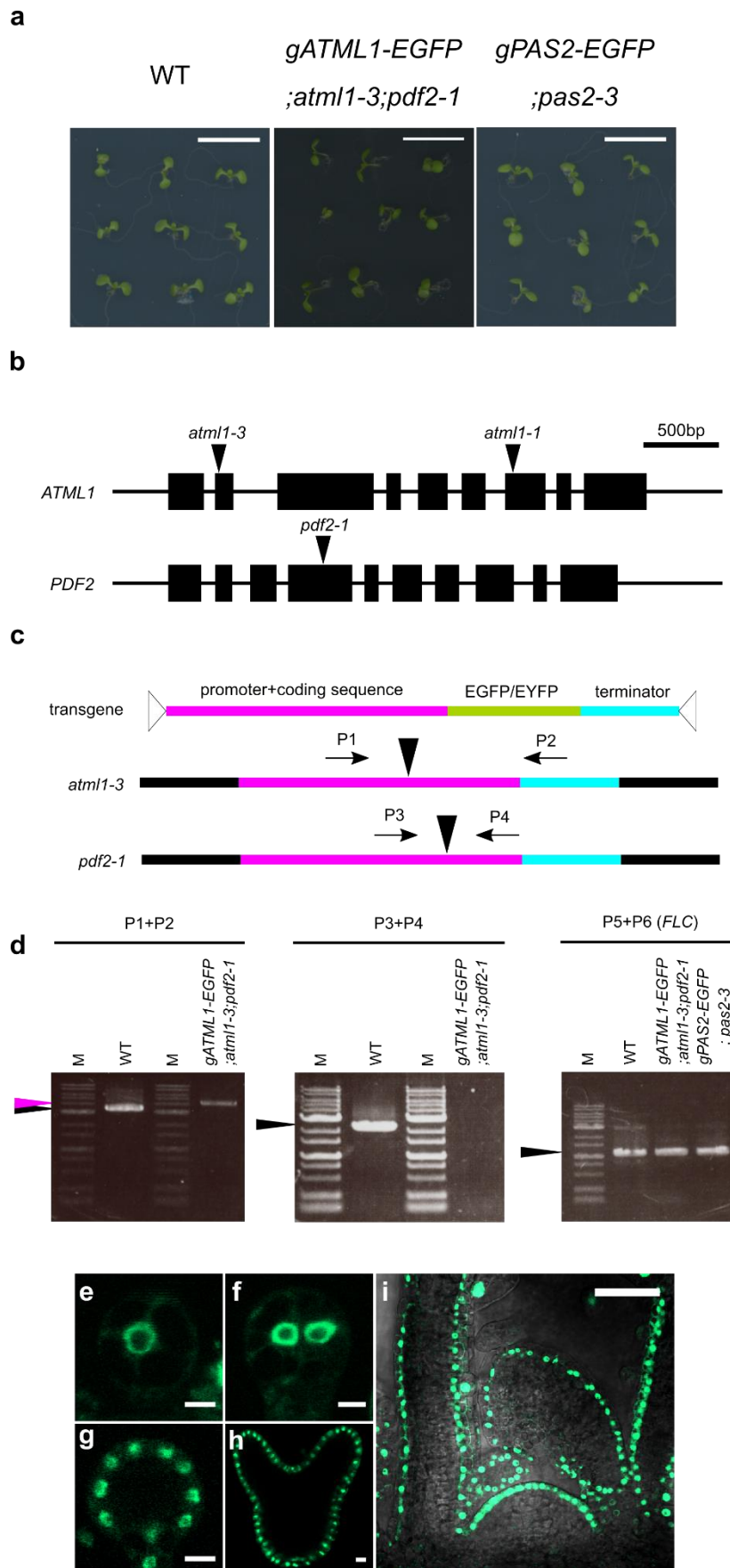
Fig. II-2 Genetic complementation with the reporter genes used in this study.

(a), Wild-type seedlings at 5 DAG (left), seedlings expressing *gATML1-EGFP* in the

atml1-3; pdf2-1 background at 5 DAG (middle), and seedlings expressing *gPAS2-EGFP*

in the *pas2-3* background at 5 DAG (right; described in the chapter-IV). **(b),** Schematic

representation of T-DNA insertion sites in mutants used in this study. **(c),** Primer design

for confirmation of mutant backgrounds in complemented seedlings (primers P1–P8;

Table 1). Arrows indicate the primer locations and arrowheads indicate the T-DNA

insertion sites. (d), Genotyping assay. Black arrow indicates the expected amplicon size

of the WT gene. A magenta arrow indicates the expected amplicon size of the transgene.

M: 1-kbp DNA Ladder. e-i, Expression of *gATML1-EGFP* during embryogenesis. (e), 1-

cell stage embryo. (f), 2-cell stage embryo. (g), Globular stage embryo. (h), Heart stage

embryo. (i), Expression of *gATML1-EGFP* in a shoot apical meristem and leaf

primordia. Scale bars: 1 cm in (a); 10 μm in (e, f); 50 μm in (g-i). (Nagata et al., 2021)

Outermost cells derived from an outermost lineage

Outermost cells derived from an inner lineage
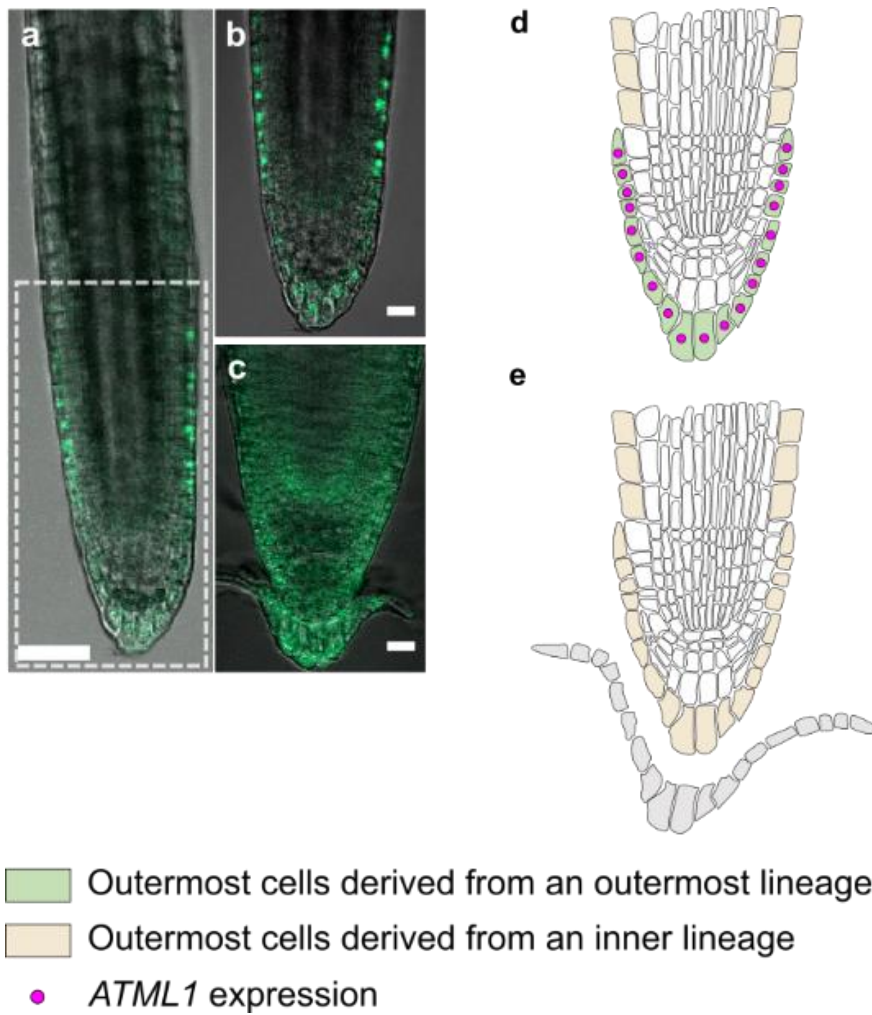
● *ATML1* expression

Fig. II-3 *ATML1* expression pattern in the primary roots.

(a), Primary root before root-cap detachment. The area surrounded by the broken line

indicates the root tip, which is shown as a magnified view in **(b). (c),** Primary root tip

after root-cap detachment. **(d, e),** Schematic representations of (a, c). The magenta circle

in schematic representations in this study indicates *ATML1* expression. Scale bars: 20

μm in (b, c); 50 μm in (a). (Nagata et al., 2021)
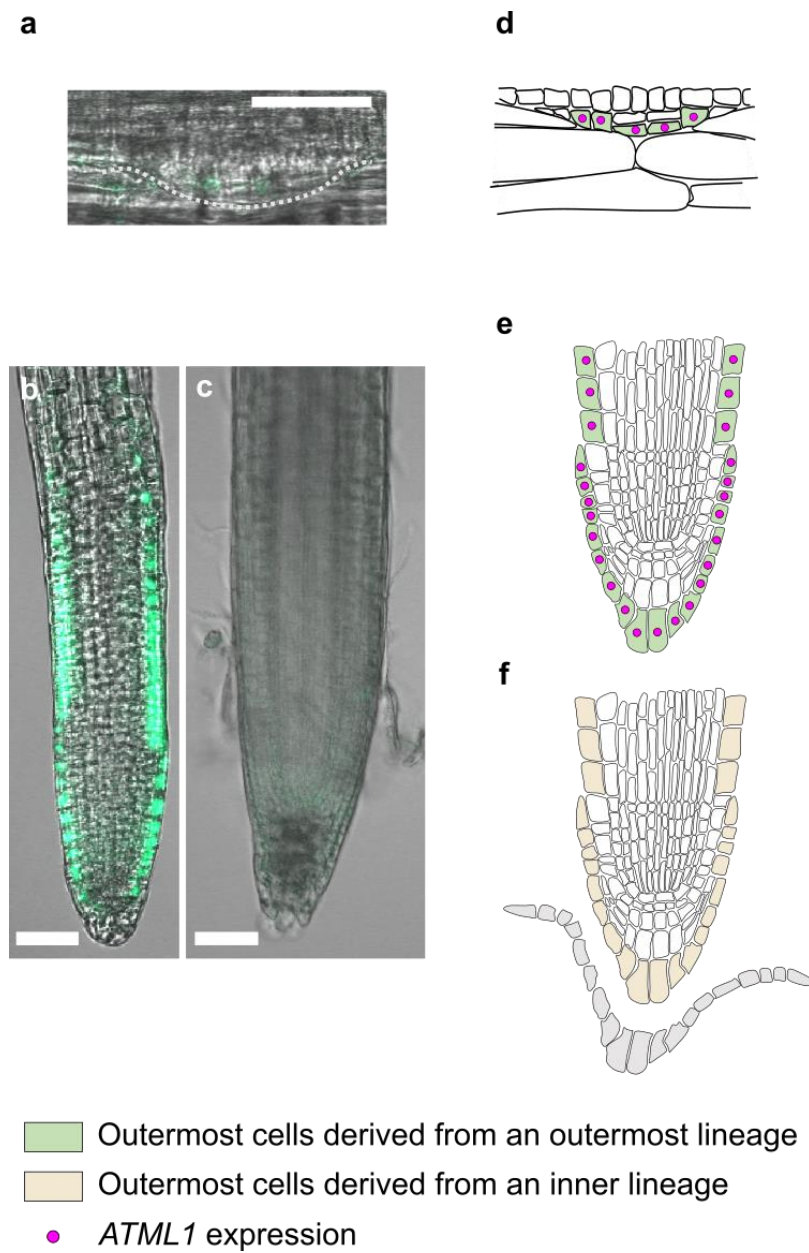
Fig. II-4 *ATML1* expression pattern during the LR development.

(a), Stage-III/IV lateral root primordia (LRPs). **(b),** Lateral root tip before root-cap detachment. **(c),** Lateral root tip after root-cap detachment. **(d-f),** Schematic representations of **(a-c).** Scale bars: 50 μm. (Nagata et al., 2021)

Fig. II-5 *ATML1* **expression pattern before and after the periclinal asymmetric division to the dermatogen stage embryo.**

(a), Octant stage embryo. **(b, c),** Two dermatogen stage embryos showing different fluorescence patterns. **(d-f),** Schematic representations of **(a-c).** Scale bars: 5 μm.

(Nagata et al., 2021)

Fig. II-6 Transgene design for a heat-inducible transient-expression system of *NLS-mCherry* and *ATML1^WT^-EGFP*.

Schematic representation of the constructs used to visualize the post-translational behavior of NLS-mCherry and ATML1^{WT}-EGFP by a heat-pulse-induced transient overexpression system. (Nagata et al., 2021)
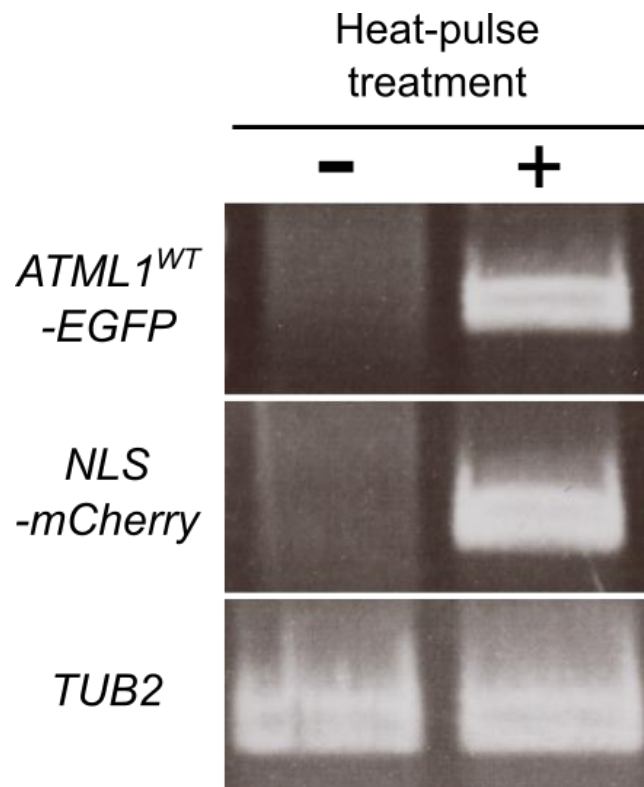
**Fig. II-7 RT-PCR analysis of mRNA extracted from the *HSP:: NLS-mCherry;*
HSP:: ATML1^{WT}-EGFP transgenic plants before and after heat-pulse treatment.**

Total RNA products were prepared from the *HSP:: NLS-mCherry; HSP:: ATML1WT-EGFP* transgenic plants before heat-pulse treatment (lane 1), and after heat-pulse treatment (lane 2). *TUB2* was used as a positive control. (Nagata et al., 2021)
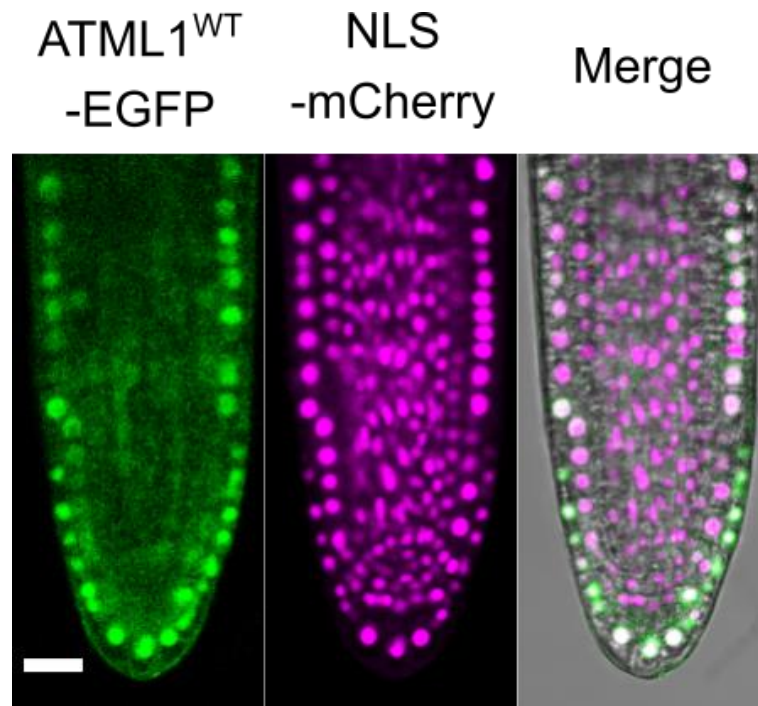
Fig. II-8 Expression patterns of systemically induced transgenes in LRs before root-cap detachment.

Fluorescence images of ATML1-EGFP (left) and NLS-mCherry (middle), and merged fluorescence and bright field image (right) in lateral roots before root-cap detachment at 2–3 hours after heat-pulse treatment. Scale bar: 20 μm. (Nagata et al., 2021)
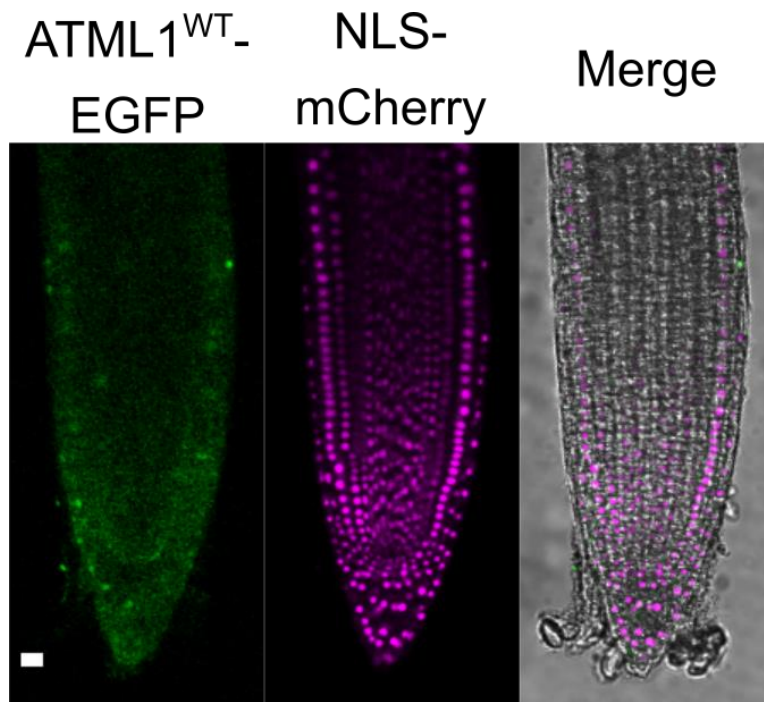
Fig. II-9 Expression patterns of systemically induced transgenes in LRs after root-cap detachment.

Fluorescence images of ATML1-EGFP (left) and NLS-mCherry (middle), and merged fluorescence and bright field image (right) in lateral roots after root-cap detachment at 2–3 hours after heat-pulse treatment. Scale bar: 20 μm. (Nagata et al., 2021)

Chapter-III

Identification of VLCFA-Cers as a lipid ligand involved in positional signaling

Introduction

In plants, Steroidogenic acute regulatory protein (StAR)-related lipid-transfer (START) domains are the common feature of the family of HD-ZIP TFs to which ATML1 and PDF2 belong (Fig. III-1) (Schrick et al., 2004; Schrick et al., 2014). START domain was first identified in a mammal (Clark et al., 1994). Mammalian proteins that contain START domain bind lipid/sterol ligands via a hydrophobic pocket, although the precise lipid ligands of plant START domain are not identified. Nevertheless, a recent study has shown that the START domains from ATML1 and PDF2 post-translationally stimulate TF activity in yeast (Schrick et al., 2014), implying that specific lipids are involved in the position-dependent functional modulation of ATML1 protein.

Furthermore, the lipid composition of the epidermis is known to be unique from other tissues (Sato, 1985; Joubes et al., 2008; Nobusawa et al., 2013). For example, epidermal cells are characterized by their waxy cuticle layer. The cuticle contains waxes as constituents, complex mixtures of hydrophobic molecules that consist of very-long-chain fatty acids (VLCFA) and their derivatives. VLCFAs synthesis is catalyzed by a four-enzyme complex associated with an endoplasmic reticulum (ER) known as the fatty acid elongase (FAE; Fig. III-2) (Li-Beisson et al., 2013). The process catalyzed by FAE is composed of four successive reactions. The first reaction is a

condensation of acyl-CoA with malonyl-CoA catalyzed by ketoacyl-CoA synthase (KCS). The second reaction is the reduction of 3-ketoacyl-CoA by 3-ketoacyl-CoA reductase (KCR). The third reaction is the dehydration of 3-hydroxy acyl-CoA by 3-hydroxy acyl-CoA dehydratase (HACD). The final step is the reduction of enoyl-CoA by enoyl-CoA reductase (ECR). Mutants that are defective for the biosynthesis of VLCFAs display pleiotropic phenotypes including abnormal morphogenesis, although defects in cuticle formation alone cannot explain all the phenotypes. Moreover, complete loss of HCD or KCR function causes embryonic lethality (Bach et al., 2008; Beaudoin et al., 2009). Thus, epidermis-specific lipids like VLCFAs may play an essential role in plant development.

Taken together, in chapter-III, I provide a detailed analysis of the role of epidermis-specific lipids in epidermis differentiation. Firstly, I examined whether the START domain of ATML1 is required for the position-dependent functional modulation of ATML1 protein. Secondly, I screened for a lipid-ligand candidate that interacts with the START domain of ATML1 and regulates the functional property of ATML1. Thirdly, I validate the role of an identified lipid ligand in *ATML1* expression.

My results strongly suggest that VLCFA-containing ceramides (VLCFA-Cer) are the ligand candidate for the START domain of ATML1 and confer the position and

lineage-dependent stability on ATML1 protein. Furthermore, based on my results, the

synthesis of epidermal-specific lipid is suggested to be not only a consequence but a

cause of epidermis differentiation.

Results

Association between the lipid-binding domain and position-dependent stability of ATML1

In Arabidopsis, 21 START domain-containing TFs comprise of HD-Zip III and IV subfamilies (Fig. III-1). These TFs are known to be involved in a variety of developmental processes. In particular, HD-Zip III subfamily contains key TFs required for vascular development, meristem initiation, and leaf polarity, while TFs of HD-Zip IV subfamily promote epidermis-related processes including trichome formation, stomatal development, and epidermis differentiation. Then, I compared the amino acid sequence of START domains from HD-Zip III and IV TFs to identify specific amino acids required for the epidermis-specific function of HD-Zip IV TFs (Fig. III-3a). In addition, to validate the importance of identified amino acids in lipid binding, I compared the amino acid sequence of START domains of ATML1 and PDF2 with the known ligand contact site of mammalian START domains (Fig. III-3b). Based on these sequence alignments, I focused on Tryptophan 471 (W471) residue, which is conserved only among HD-Zip IV TFs and exhibits strong similarity with the ligand contact site of mammalian START domains, as a putative lipid contact site (Fig. III-3).

To analyze the function of W471 in the position-dependent functional

modulation of ATML1, I introduced a W471L point mutation into ATML1 based on the

previous study by using site-directed mutagenesis methods and generated transgenic

plants harboring the transient induction system of *ATML1^{W471L}-EGFP* and *NLS-mCherry* (Fig. III-4). Heat-pulse induction of the transcription of both *ATML1^{W471L}-EGFP* and *NLS-mCherry* was confirmed by RT-PCR analysis (Fig. III-5). Consistent

with the observations as described in chapter-II, the fluorescence of mCherry was

observed equally in all cells in young LRs after heat treatment (Fig. III-6). However, in

contrast to ATML1^{WT}-EGFP, transient induction of ATML1^{W471L}-EGFP in young LRs

led to the disappearance of fluorescence in the outermost cells (Fig. III-6).

該当部分に関して、5 年以内に雑誌で刊行予定のため、非公開。

該当部分に関して、5 年以内に雑誌で刊行予定のため、非公開。

該当部分に関して、5 年以内に雑誌で刊行予定のため、非公開。

Identification of VLCFA-Cers as a lipid ligand candidate involved in positional

signaling

My results mentioned above strongly suggest that W471 residue in the START domain

is crucial for the cell position and lineage dependent stability of ATML1 protein in the

outermost cells and plays a role in the protein-protein interaction of ATML1. Therefore,

I hypothesized that the positional signaling molecule or its downstream product directly

binds to the START domain, altering the functional property of ATML1. Thus, I

performed *in vitro* protein-lipid overlay (PLO) assays to identify lipid species that interact with the ATML1 START domain. I found that the recombinant GST-tagged START domain of ATML1 bound to VLCFA-containing ceramides (VLCFA-Cers), ceramide-1-phosphatates (C1Ps), phosphatidic acids, phosphatidylserines (PSs), and several phosphatidylinositol phosphates (Fig. III-10, 11). In these assays, GST-START showed no binding affinity for other plant sphingolipid species, cholesterol, mammalian glycolipid species, and other biological important lipids (Fig. III-10, 11, 12).

Next, I evaluated the effect of the W471L mutation on the lipid-binding ability of the START domain. Because the results obtained from a PLO assay are qualitative, the changes in interaction affinity between ATML1 and lipid were deduced by comparing the signal intensity of subjected lipid with that of C24 C1P (originally prepared sphingolipid strips) or with that of PS (PIP strips). I thus revealed that the W471L mutation specifically attenuated the interaction between GST-START and VLCFA-Cers (Fig. III-10, 11).

To determine whether or not the stability of ATML1 is affected by VLCFA-Cers, I treated *HSP::NLS-mCherry; HSP::ATML1^{WT} –EGFP* seedlings with cafenstrole, which inhibits the activity of b-ketoacyl-CoA synthase required for VLCFA biosynthesis (Fig. III-2), and observed EGFP fluorescence in young LRs. The pool of ceramides and

complex sphingolipid in plants treated with cafenstrole for 5 DAG showed a significant

decrease in fatty acids with chain lengths of 24 or more carbon atoms and a significant

increase in fatty acids with chain lengths of 22 or fewer carbon atoms, confirming the

effects of cafenstrole on the VLCFA-Cer synthesis (Fig. III-13). In the presence of

cafenstrole, the disappearance of the fluorescence of ATML1^{WT}-EGFP was observed in

outermost cells derived from the outermost lineage after heat-pulse induction (Fig. III-

14), similar to my observations for *HSP::NLS-mCherry;HSP::ATML1^{W471L} –EGFP*

(Fig. III-6). Moreover, treatment with cafenstrole strongly reduced both the fluorescence

intensity of EGFP and the number of outermost cells expressing ATML1-EGFP in

gATML1-EGFP seedlings (Fig. III-15).

Involvement of VLCFA-Cers in the positive feedback regulation of *ATML1* and

PDF2

The observed effect of VLCFA-Cers on the stability of ATML1 suggests that VLCFA-

Cers might affect the regulation of *ATML1* and *PDF2* via a positive feedback

mechanism. To assess this hypothesis, I examined the transcription level of *ATML1* and

PDF2 in wild-type plants treated with cafenstrole for 5 DAG and found that cafenstrole

treatment strongly reduced the amount of *ATML1* mRNA and *PDF2* mRNA by

quantitative RT-PCR analysis (Fig. III-16).

To exclude the possibility that these effects are due to the side-effect of cafenstrole treatment rather than the decrease in the amount or proportion of VLCFA in the fatty acid pool of ceramides and complex sphingolipids, the effect of fumonisin B1(FB1) treatment, which inhibits the activity of ceramide synthases that preferentially use VLCFA as a substrate (Fig. III-10a), was examined. Consistent with the previous research, the pool of ceramides and complex sphingolipid in plants treated with FB1 for 5 days showed not only a significant decrease in fatty acids with chain lengths of 22 or more carbon atoms but a great increase in fatty acids with chain lengths of 20 or fewer carbon atoms, decreasing the proportion of VLCFA in fatty acid pool of ceramides and complex sphingolipids (Fig.III-17).

該当部分に関して、5 年以内に雑誌で刊行予定のため、非公開。

Quantitative RT-PCR analysis revealed that FB1 treatment also greatly reduced the mRNA levels of *ATML1* and *PDF2* genes (Fig.III-18). Collectively, these expression analyses indicate that VLCFA-Cers function as an essential component of a positive feedback loop involving ATML1 and PDF2.

Discussion

In the former half of this chapter, I focused on and analyzed the function of Tryptophan 471 (W471) residue of the START domain of ATML1. The previous report has shown that START domains from several mammalian proteins and several plant HD-Zip proteins can stimulate TF activity when these START domains are embedded within a synthetic TF in yeast (Schrick et al., 2014).

Amino acid sequence alignment analysis showed that the W471 residue was conserved only among HD-Zip IV TFs (Fig. III-3). Furthermore, the W471 residue corresponds to and exhibits strong similarity with the F266 residue of mammalian StAR protein (Fig. III-3). The F266 residue of mammalian StAR protein is located in the 4th α-helix and predicted as a ligand contact site (Schrick et al., 2014). In functional analysis of specific amino acids within the START domain of the mammalian StAR protein, the F266L mutation strongly disrupts its ability to modulate the TF activity (Schrick et al., 2014). Given these findings, I focused on the W471 residue as a putative ligand contact site essential for the epidermis-specific function of the START domain of ATML1.

Interestingly, the W471L mutation led to the rapid degradation of ATML1 protein even in the outermost cells (Fig. III-6). This result suggests that signal perception for which the W471 residue is required is crucial for the post-translational

regulation of ATML1 in the outermost cells.

該当部分に関して、5 年以内に雑誌で刊行予定のため、非公開。

該当部分に関して、5 年以内に雑誌で刊行予定のため、非公開。

In the latter half of this section, I focused on VLCFA-Cers as a ligand candidate for ATML1 and analyzed its role in ATML1 expression. I found that the START domain of ATML1 binds to a broad range of lipid classes, whereas the W471L mutation specifically attenuated the interaction between GST-START and VLCFA-Cer (Fig. III-10, 11). Therefore, VLCFA-Cer is a candidate ligand for ATML1 which is required for its TF activity.

The complete loss of VLCFAs or VLCFA-sphingolipids results in embryonic lethality (Bach et al., 2008; Markham et al., 2011), implying their crucial roles in plant development. Thus, I performed physiological and genetical analyses using two inhibitors, cafenstrole and FB1 that can perturb the biosynthesis of VLCFA-Cers (Trenkamp et al., 2004; Markham et al., 2011; Nobusawa and Umeda, 2012; Luttgeharm et al., 2016), in order not to mistake the side-effects for the effects caused by the reduction of the amount of VLCFA-Cers. Cafenstrole, a carbamoyl sulfonyl triazole herbicide, blocks the first reaction in VLCFA elongation by targeting KCS (Trenkamp et al., 2004; Nobusawa and Umeda, 2012). VLCFA reduction induced by

cafenstrole treatment results in pleiotropic effects including fused leaves which is also

caused by defects in the formation of the cuticle (Nobusawa and Umeda, 2012;

Nobusawa et al., 2013). On the other hand, FB1, a virulence factor produced by several

species of *Fusarium* molds whose infections induce programmed cell death (PCD),

blocks a more specific reaction for the biosynthesis of VLCFA-Cers by targeting LAG

ONE HOMOLOGUE 1 (LOH1) and LOH3 ceramide synthases which catalyze the

incorporation of VLCFAs into sphingolipids (Markham et al., 2011;Berkey et al., 2012).

Arabidopsis treated with FB1 results in various morphological and physiological defects

including the accumulation of long-chain bases (LCBs), which triggers PCD (Markham

et al., 2011; Berkey et al., 2012). To avoid the excess induction of PCD, long-term FB1

treatment was performed at a moderate concentration based on the recent studies

(Markham et al., 2011).

該当部分に関して、5 年以内に雑誌で刊行予定のため、非公開。

Plant sphingolipids can vary in the composition of their head groups, degree of

hydroxylation in fatty acids and LCBs, numbers and positions of double bonds in fatty

acids and LCBs, and the length of fatty acids. Such a structural diversity is fundamental

to diverse microdomains with distinct functions (Jarsch et al., 2014; Lv et al., 2017). For

example, fatty acids can be 2-hydroxylated by two fatty acid 2-hydroxylases, FAH1 and

FAH2, and this modification is shown to be crucial to the formation of the

microdomains (Nagano et al., 2016). In *Osfah1/2* plants, an organization of various

defense proteins localized in the microdomains is disturbed (Nagano et al., 2016). On

contrary, in plants overexpressing AtBI-1 which interacts with FAH1 and FAH2,

GlcCers containing 2-hydroxylated fatty acids accumulate in the microdomains and

microdomain-specific localizations of proteins involved in plant defense are disrupted

(Ishikawa et al., 2015).

Furthermore, ceramide as a second messenger can be generated through the

sphingomyelinase pathway (Fig. III-10) (Kitatani et al., 2008; Pata et al., 2010;

Stancevic and Kolesnick, 2010; Merrill Jr, 2011). Although an equivalent pathway is not

yet identified in plants, in the sphingomyelinase pathway that occurs in the plasma

membrane, ceramides are generated through sphingomyelinase (SMase)-dependent

catabolism of sphingomyelin (SM), initiating intra-cellular ceramide signaling. In

addition, the activity of SMase is commonly exerted in the microdomain and regulated

by the microdomain composition (Silva et al., 2009).

As described above, the fine-tuning of the sphingolipid synthesis is critical for

the formation of various microdomains, the functions of microdomain-specific proteins,

and the generation of ceramide as a second messenger. I found that FB1 treatment

reduced the mRNA levels of *ATML1* and *PDF2* in wild-type plants as well as

cafenstrole treatment, although the effects seem to be specific to several ceramide

species. I propose two hypotheses for the reduced mRNA levels of *ATML1* and *PDF2* in

wild-type plants treated with FB1: (i) FB1 treatment directly reduces the amount of the

specific VLCFA-Cers which is the authentic ligand of ATML1 and PDF2, (ii) the altered

proportion of each sphingolipid classes affects the microdomain composition, affecting

the accessibility toward VLCFA-Cers generated via the SMase-like pathway. Thus,

identification of the authentic lipid ligand for ATML1 and the enzymes involved in the

catabolism of complex sphingolipids might be required for further studies.

Fig. III-1 Schematic diagrams of the representative protein structures of HD-Zip III TFs (top) and HD-Zip IV TFs (bottom).

HD, homeodomain; LZ, leucine zipper; START, steroidogenic acute regulatory protein (StAR)-related lipid transfer domain; SAD, START adjacent domain; MEKHLA, MEKHLA domain.
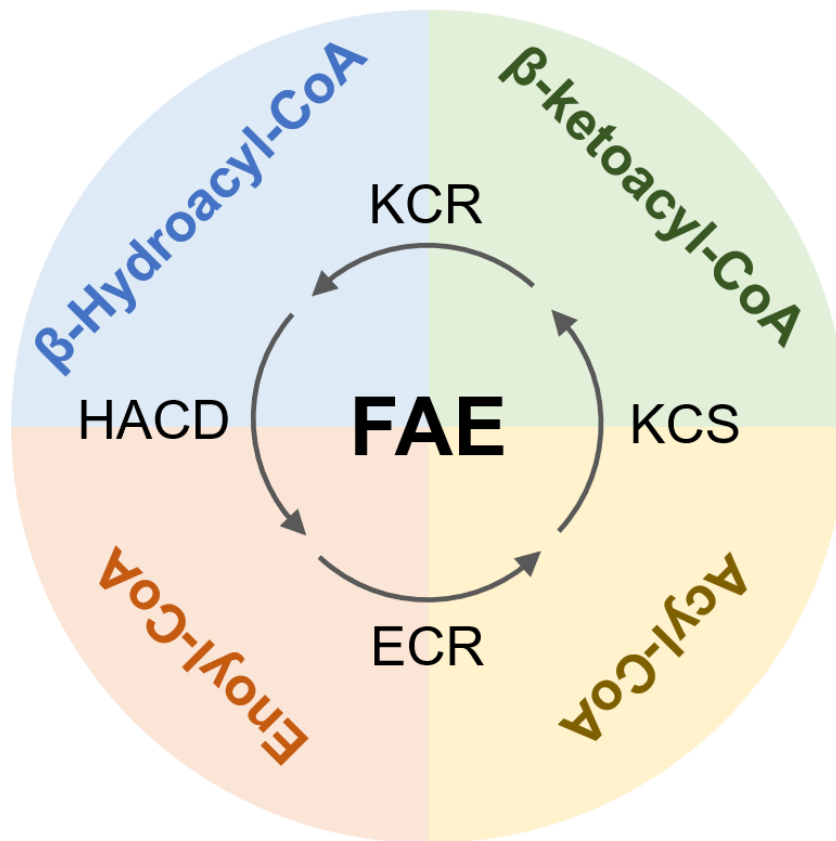
Fig. III-2 Schematic representation of the reaction of fatty acid elongation catalyzed by fatty acid elongase (FAE) complex.

Sequential activities of four enzymes (KCS, KCR, HACD, and ECR) that comprise fatty acid elongase (FAE) complex elongate saturated C18 fatty acids produced in the plastid by adding a two-carbon unit to the carboxy terminal repeatedly.
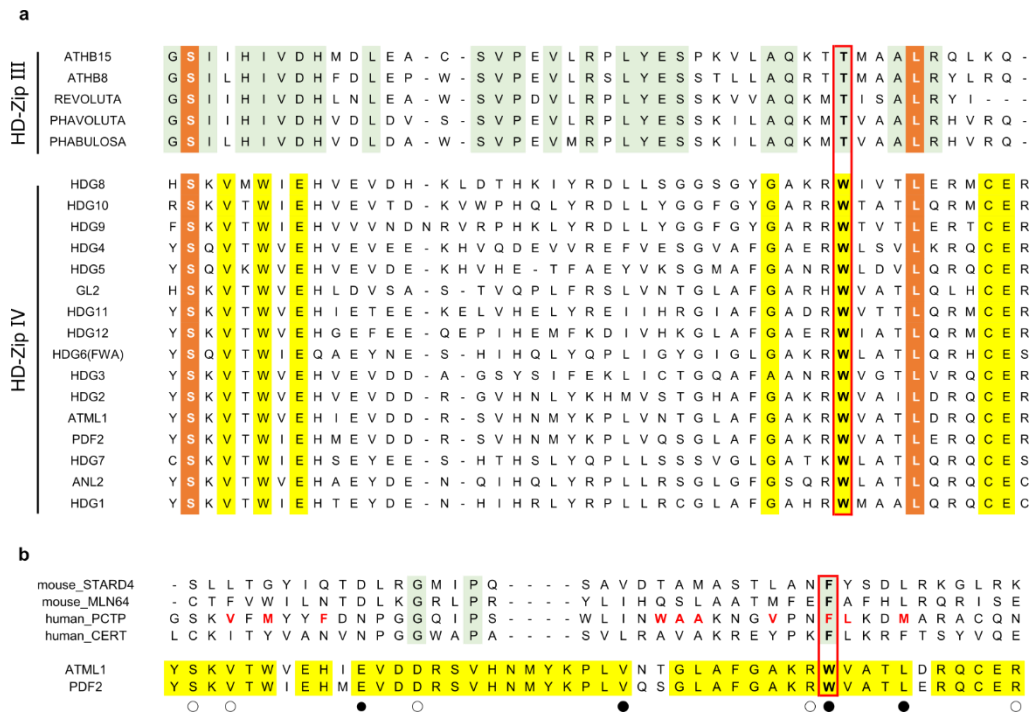
Fig. III-3 Amino acid sequence alignment of the C-terminal regions of the START domain containing proteins.

(a), Amino acid sequence alignment of the C-terminal region of the START domain from HD-Zip IV and HD-Zip III proteins. (b), Amino acid sequence alignment of the C-terminal regions of the START domains from STARD4, MLN64, PCTP, CERT, ATML1, and PDF2. Red font indicates ligand contact points, as derived from the PCTP-PtCho co-crystal. The amino acid targeted for site-directed mutagenesis of ATML1 is indicated by the red box. The yellow background color indicates amino acids conserved in HD-Zip IV proteins but not in HD-Zip III proteins (a), or in ATML1 and PDF2, but not in mammalian proteins (b). The green background color indicates amino acids

75

conserved in HD-Zip III proteins but not in HD-Zip IV proteins (a), or in mammalian

proteins but not in ATML1 or PDF2 (b). The orange background color indicates amino

acids conserved among HD-Zip III proteins and HD-Zip IV proteins. Open circles

indicate the sites where the amino acids exhibit weak similarity. Closed circles indicate

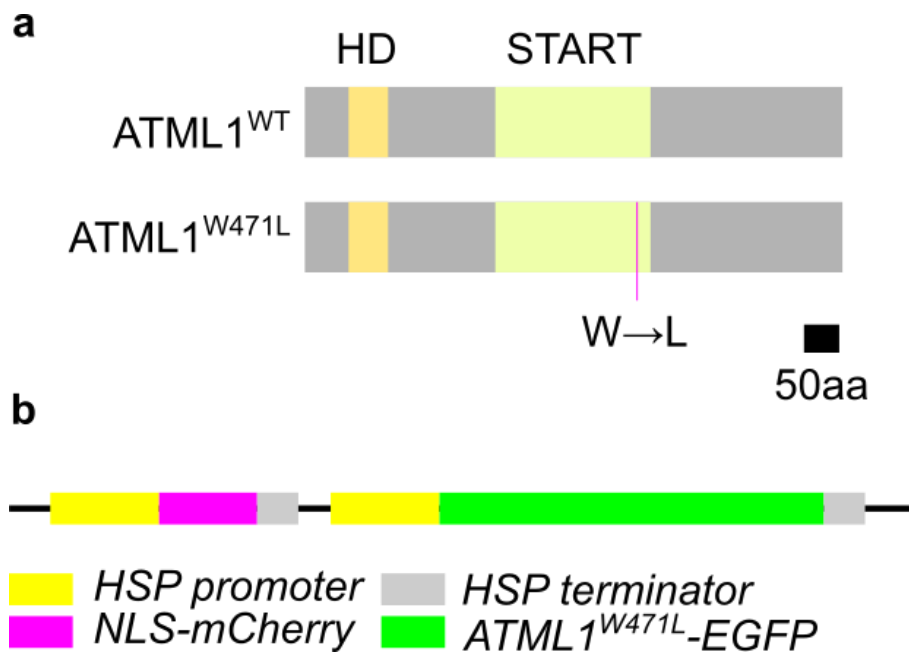the sites where the amino acids exhibit strong similarity. (Nagata et al., 2021)

Fig. III-4 Transgene design for a heat-inducible transient-expression system of

***NLS-mCherry* and *ATML1^{W471L}-EGFP*.**

(a), Schematic diagram of wild-type ATML1 (top) and ATML1^{W471L} (bottom) protein

structures. HD, homeodomain; START, steroidogenic acute regulatory protein (StAR)-

related lipid transfer domain. The magenta line indicates the site-directed mutagenesis

site. (b), Schematic representation of the constructs used to visualize the post-

translational behavior of NLS-mCherry and ATML1^{WT}-EGFP by a heat-pulse-induced

transient overexpression system. (Nagata et al., 2021)
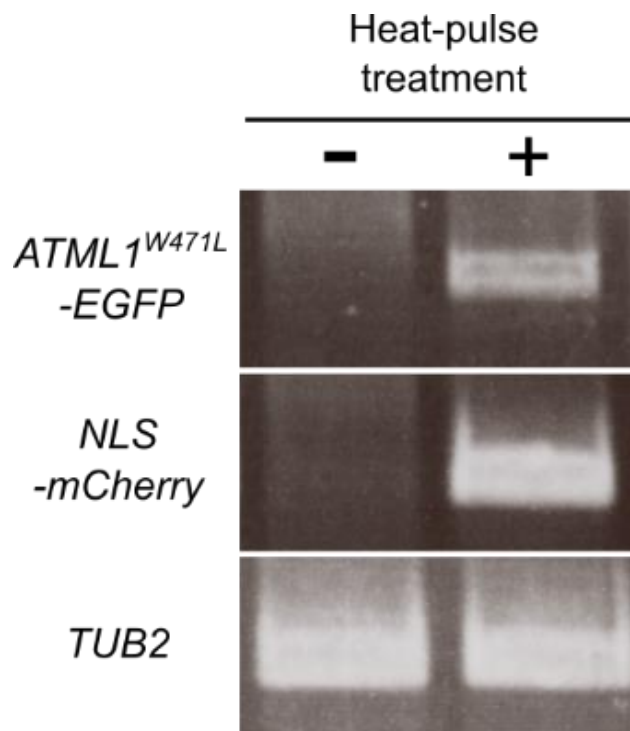
Fig. III-5 RT-PCR analysis of mRNA extracted from the *HSP:: NLS-mCherry;*

***HSP:: ATML1^{W471L}-EGFP* transgenic plants before and after heat-pulse treatment.**

Total RNA products were prepared from the *HSP:: NLS-mCherry; HSP:: ATML1^{W471L}-EGFP* transgenic plants before the heat-pulse treatment (lane 1), and after the heat-pulse treatment (lane 2). *TUB2* was used as a positive control. (Nagata et al., 2021)
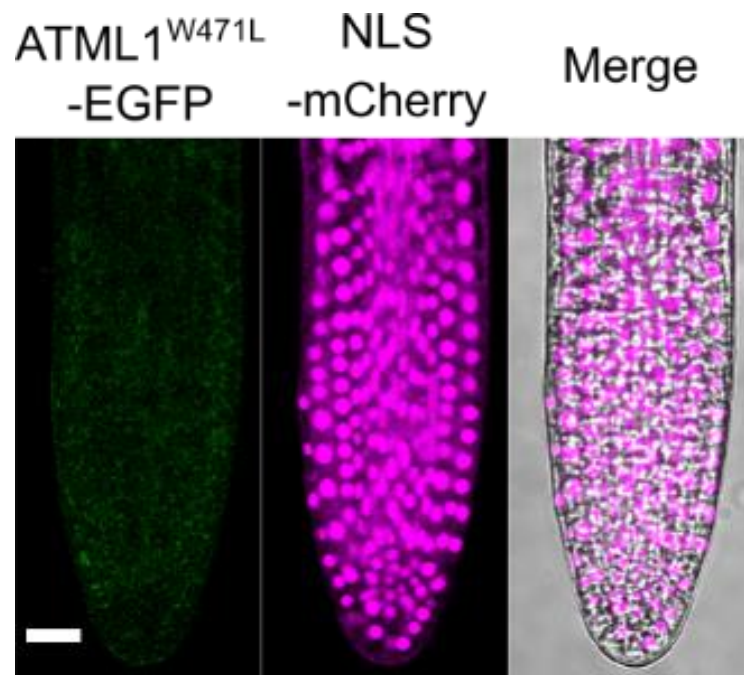
Fig. III-6 Expression patterns of systemically induced transgenes in a LR before root-cap detachment.

Fluorescence images of ATML1^{W471L}-EGFP (left) and NLS-mCherry (middle), and merged fluorescence and bright field image (right) in a LR before root-cap detachment at 2–3 hours after heat-pulse treatment. Scale bar: 20 μm. (Nagata et al., 2021)

該当部分に関して、5 年以内に雑誌で刊行予定のため、非公開。

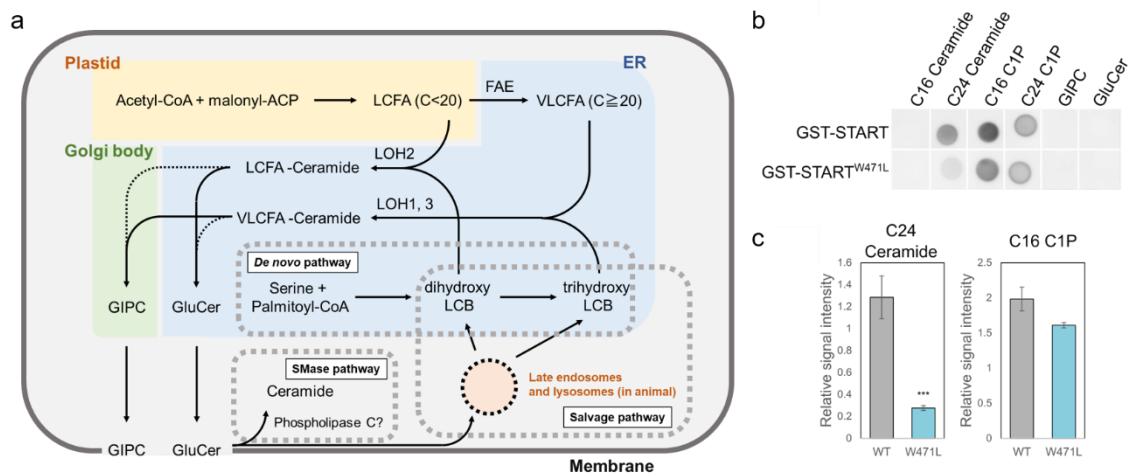該当部分に関して、5 年以内に雑誌で刊行予定のため、非公開。

該当部分に関して、5 年以内に雑誌で刊行予定のため、非公開。

Fig. III-10 Protein–lipid interaction between ATML1^{WT} or ATML^{W471L} and plant sphingolipids.

(a), Schematic overview of the sphingolipid biosynthesis pathway in plants. **(b),**

Interactions of the GST-tagged START domain of ATML1 (GST-START) and

ATML1^{W471L} (GST-START^{W471L}) with plant sphingolipids observed by protein–lipid

overlay (PLO) assay. **(c),** Relative signal intensity of protein–lipid interaction observed

by PLO assay. C24 ceramide (left) and C16 C1P (right). Data are mean ± SE values

(***$P < 0.01$, Student's t test, n = 5 for PLO assay using GST-START and n = 3 for

PLO assay using GST-START^{W471L}). C16 C1P, C16 ceramide-1-phosphate; C24 C1P,

C24 ceramide-1-phosphate; ER, endoplasmic reticulum; GIPC, glycosyl inositol

phosphoceramide; GluCer, glucosylceramide. (Nagata et al., 2021)

Fig. III-11 Protein–lipid interaction between ATML1$^{\text{WT}}$ or ATML$^{\text{W471L}}$ and all phosphoinositides and several other biological important lipids.

(a), Interactions of the GST-tagged START domain of ATML1 (GST-START) and ATML1$^{\text{W471L}}$ (GST-START$^{\text{W471L}}$) with all phosphoinositides and several other biological important lipids by protein–lipid overlay (PLO) assay. **(b),** Relative signal intensity of protein–lipid interaction observed by PLO assay. Data are mean ± SE values (***$P <$ 0.01, Student's t test, n = 5 for PLO assay using GST-START and n = 3 for PLO assay using GST-START$^{\text{W471L}}$). LPA, Lysophosphatidic acid; LPC, Lysophosphocholine;

PtdIns, Phosphatidylinositol; PtdIns(3)P, Phosphatidylinositol (3)-phosphate; PtdIns(4)P, Phosphatidylinositol (4)-phosphate; PtdIns(5)P, Phosphatidylinositol (5)-phosphate; PE, Phosphatidylethanolamine; PC, Phosphatidylcholine; S1P, Sphingosine 1-Phosphate; PtdIns(3,4)P2, Phosphatidylinositol (3,4)-bisphosphate; PtdIns(3,5)P2, Phosphatidylinositol (3,5)-bisphosphate; PtdIns(4,5)P2, Phosphatidylinositol (4,5)-bisphosphate; PtdIns(3,4,5)P3, Phosphatidylinositol (3,4,5)-trisphosphate; PA, Phosphatidic acid; PS, Phosphatidylserine. (Nagata et al., 2021)
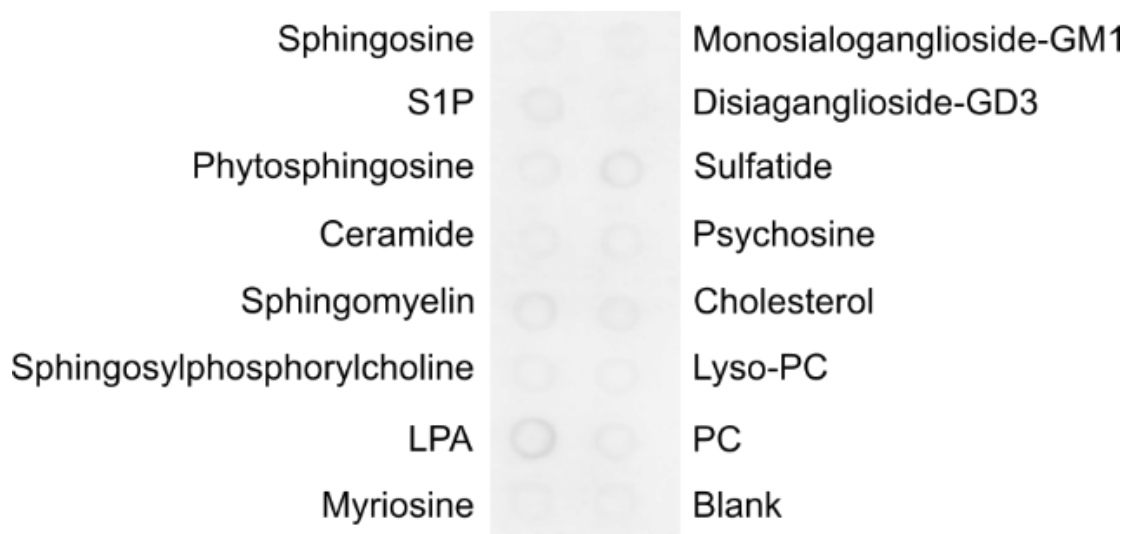
Fig. III-12 Protein–lipid interaction between ATML1^{WT} and various sphingolipids or several other lipids.

(a), Interactions of the GST-tagged START domain of ATML1 (GST-START) with various sphingolipids and several other lipids by protein–lipid overlay (PLO) assay.

S1P, Sphingosine 1-phosphate; LPA, Lysophosphatidic Acid; Lyso-PC, Lysophosphatidylcholine; PC, Phosphatidylcholine. (Nagata et al., 2021)

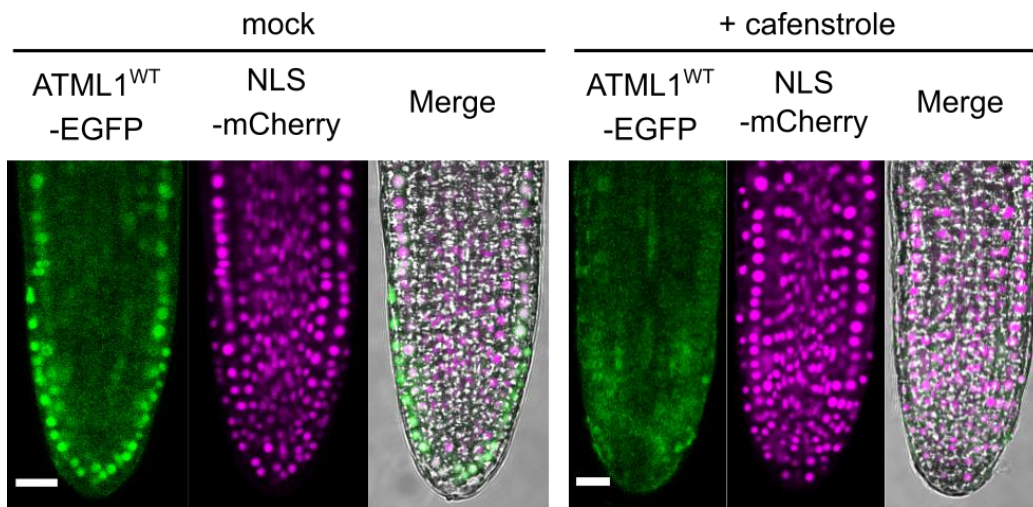該当部分に関して、5 年以内に雑誌で刊行予定のため、非公開。

該当部分に関して、5 年以内に雑誌で刊行予定のため、非公開。

Fig. III-14 Expression patterns of systemically induced transgenes in LRs before root-cap detachment with mock or cafenstrole treatment.

Fluorescence images of ATML1^{WT}-EGFP (left) and NLS-mCherry (middle), and merged fluorescence and bright field image (right) in LRs before root-cap detachment at 2–3 hours after heat-pulse treatment with mock or 0.3 µM cafenstrole treatment. Scale bar: 20 µm. (Nagata et al., 2021)
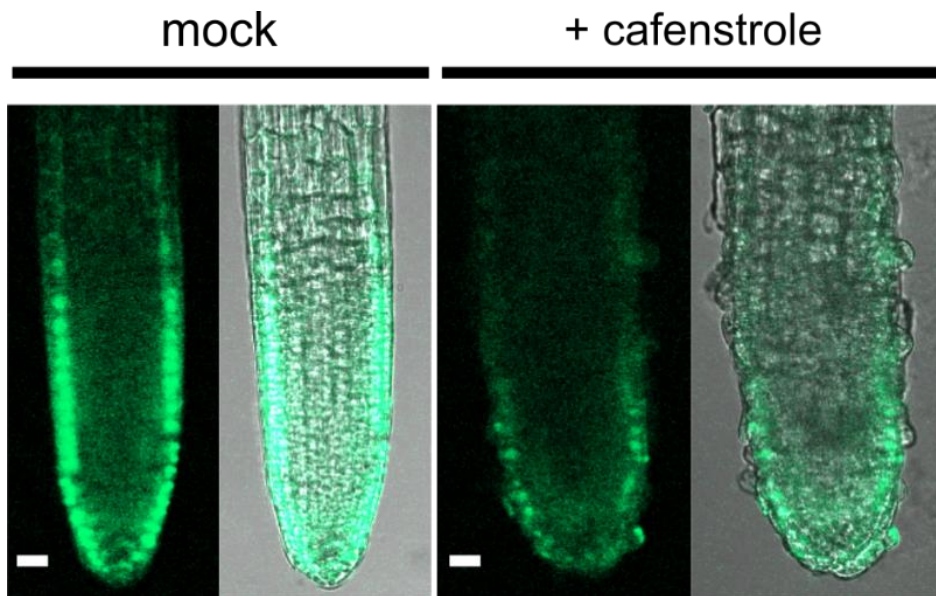
Fig. III-15 Expression patterns of *gATML1-EGFP* in LRs before root-cap detachment with mock or cafenstrole treatment.

Fluorescence images of ATML1-EGFP (left) and merged fluorescence and bright field image (right) in LRs before root-cap detachment with mock or 0.3 μM cafenstrole treatment. Scale bar: 20 μm. (Nagata et al., 2021)
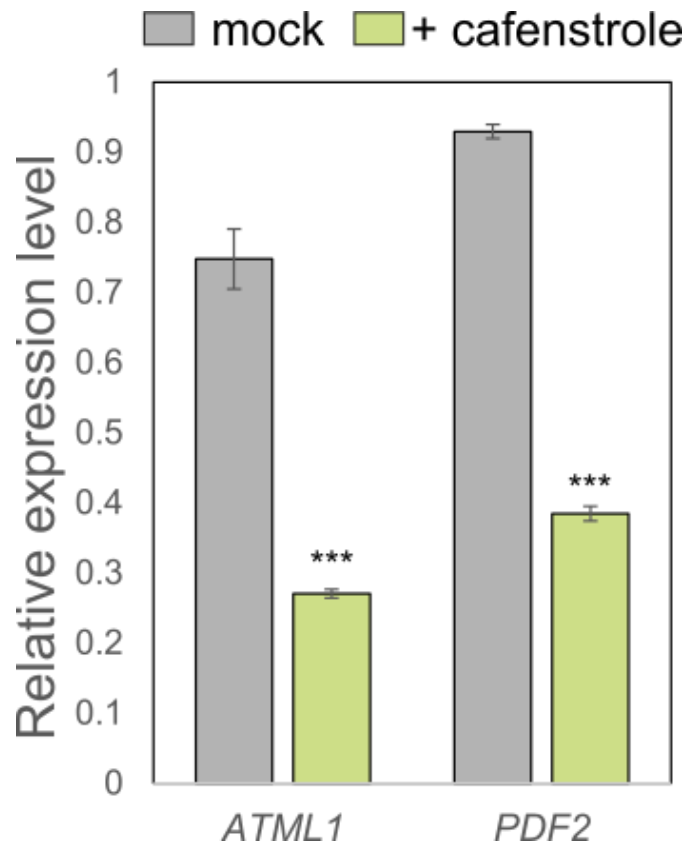
Fig. III-16 Relative expression levels of *ATML1* and *PDF2* in 5 DAG wild-type seedlings with mock or cafenstrole treatment.

Total RNA was prepared from 5 DAG wild-type seedlings with mock or 0.3 μM cafenstrole treatment. Data are mean ± SE values (***$P < 0.01$, Student's t test, n = 3).

(Nagata et al., 2021)

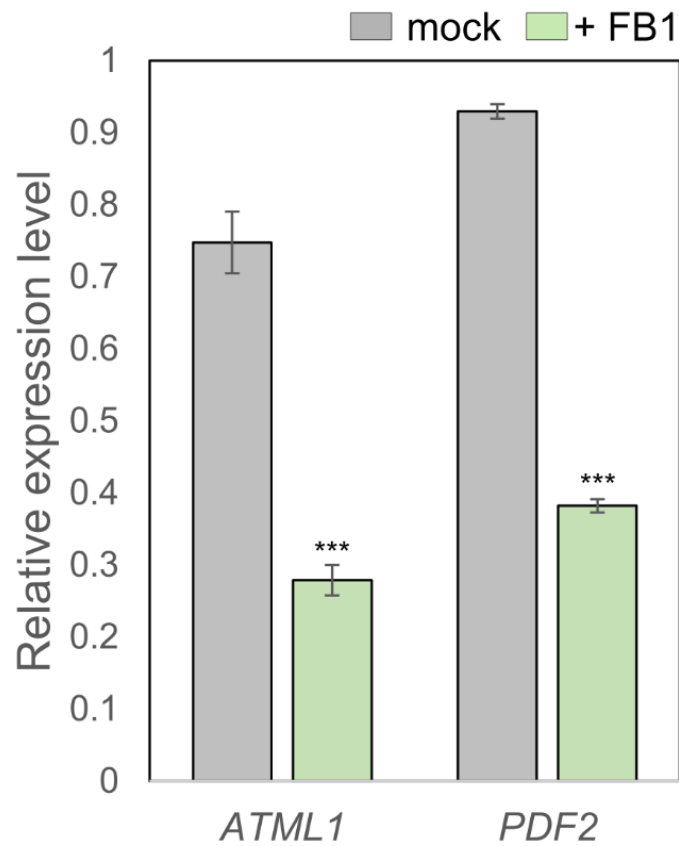該当部分に関して、5 年以内に雑誌で刊行予定のため、非公開。

該当部分に関して、5 年以内に雑誌で刊行予定のため、非公開。

Fig. III-18 Relative expression levels of *ATML1* and *PDF2* in 5DAG WT seedlings with mock or FB1 treatment.

Total RNA was prepared from 5 DAG WT seedlings with mock or 0.5 μM FB1 treatment. Data are mean ± SE values (***$P < 0.01$, Student's t test, n = 3). (Nagata et al., 2021)

Chapter-IV

Analysis of the regulation of VLCFA-Cer synthesis and localization

Introduction

The asymmetric cell division (ACD) is a common mechanism for generating cellular diversity. In Arabidopsis, stomatal development, which starts with ACD of a meristemoid mother cell (MMC) to generate a meristemoid and a stomatal lineage ground cell (SLGC), provides a representative example of the ACD-based cell-fate determination (Fig. IV-1). BREAKING OF ASYMMETRY IN THE STOMATAL LINEAGE (BASL), localizing in the plasma membrane distal to the future division plane of the MMC, is a key protein in the ACD-based cell fate assignment in the stomatal cell lineage (Dong et al., 2009; Zhang et al., 2015; Zhang et al., 2016).

The polarized localization of BASL is stabilized by its phosphorylation that is regulated by a mitogen-activated protein kinase (MAPK) signaling cascade, and in turn, phosphorylated BASL recruits the MAPK signaling as a scaffold. Thus, the BASL-MAPK signaling feedback loop is reinforced in a polarized manner, and hence the MAPK signaling asymmetrically phosphorylates SPEECHLESS (SPCH) that is required for stomatal differentiation, resulting in SPCH degradation and inhibition of progression of the stomatal fate only in the SLGC.

Similarly, I observed the ACD-based protodermal-cell fate determination during the embryogenesis (Fig. II-5). Furthermore, I proposed that this asymmetric cell-

fate determination is due to the outermost-cell specific formation of ATML1-VLCFA-Cer complex. Because the ATML1 protein itself was segregated to both the inner and outermost cells after ACDs, VLCFA-Cer may be asymmetrically localized in the plasma membrane before ACDs.

In mammalian polarized epithelial cells, a lipid raft-based apical sorting and trafficking results in sphingolipid-rich apical membrane compartmentation, generating the inner-outer cell polarity (Fig. IV-2) (Simons and Ikonen, 1997; Surma et al., 2012). Similarly, plasma membranes of the plant epidermal cells are also known to be polarized and compartmentalized (Fig. IV-2) (Watanabe et al., 2004; Luo et al., 2007; Nakamura and Grebe, 2018), implying the involvement of specific sphingolipids in the polarity establishment of the plant epidermal cells.

In chapter-IV, I provide a detailed analysis of the VLCFA-Cer synthesis site in relation to the *ATML1* expression and the epidermal cell polarity. Firstly, I observed the spatial expression patterns of essential enzymes for the VLCFA-Cer synthesis. Secondly, I examined the epistatic relationship between VLCFA-Cer and ATML1. Thirdly, I investigated the localization of VLCFA-Cer in the epidermal cells. My results strongly suggest that epidermal cells are the primary site for the VLCFA-Cer synthesis, and a positive feedback loop involving ATML1 and VLCFA-Cer is present.

Furthermore, the epidermal cell polarity is dependent on VLCFA-sphingolipid-based

apical sorting and trafficking, suggesting that the generation of VLCFA-Cers occurs at

the apical membrane that faces the environment.

Results

Characterization of the VLCFA-Cer synthesis site

I analyzed the expression pattern of PASTICCINO2 (PAS2) which encodes HCD that is

essential for VLCFA synthesis (Fig. III-2). Although homozygous *pas2–3* mutants

exhibit an embryonic lethal phenotype, genetic complementation of *pas2-3* by

transgenic expression of a genomic reporter restored mutants to growth

indistinguishable from wild-type plants (Fig. II-2). In *gPAS2-EGFP; pas2-3* plants, the

fluorescence of PAS2-EGFP was restricted to the outermost cells as well as that of

ATML1 (Fig. IV-3, 4). In contrast to ATML1, the fluorescence of PAS2-EGFP was

observed even in the outermost cells of roots after the detachment of root cap cells (Fig.

IV-5a). Furthermore, consistent with a previous study, the fluorescence of PAS2-EGFP

was also observed in the endodermis (Fig. IV-5b). Because VLCFAs are essential

precursors of aliphatic suberins in roots, this *PAS2* expression in the endodermis likely

contributes to root suberin biosynthesis.

該当部分に関して、5 年以内に雑誌で刊行予定のため、非公開。

A previous study has shown that gene silencing of *PDF2* and *ATML1*

downregulates the mRNA levels of VLCFA biosynthesis-related genes (Rombola-

Caldentey et al., 2014). The expression pattern of PAS2 together with the presence of an

L1-box sequence in the *PAS2* promoter implies that VLCFA-Cers biosynthesis in the

outermost cells is activated via transcriptional activation by a positive-feedback loop

involving ATML1 and PDF2. Consistently, the sphingolipid pool in viable hypomorphic

atml1-1; pdf2-1 plants showed a significant decrease in VLCFA-Cers (Fig. IV-7).

VLCFA-sphingolipids-mediated compartmentation of the apical membrane

Previous studies have shown that some membrane proteins, such as the ATP-binding

cassette transporter ABCG11/WBC11, are located exclusively in the apical membrane

of epidermal cells that faces the external environment (Luo et al., 2007; Panikashvili

and Aharoni, 2008), whereas I found that Remorin 1.2 (REM1.2) (Jarsch et al., 2014) is

localized to the basolateral membrane of the epidermal cells (Fig. IV-8). I therefore

explored whether apical membrane compartmentation requires VLCFA-Sphingolipids

by analyzing the effects of FB1 treatment based on the recent study (Markham et al.,

2011). At 24 hours after FB1 treatment, the fluorescence of WBC11 was internalized in

LR epidermal cells, whereas the fluorescence of REM1.2 was not affected (Fig. IV-8).

Taken together, these results suggest that VLCFA-Sphingolipids play a role in

establishing the apical membrane compartments of epidermal cells.

Discussion

Because the ATML1-VLCFA-Cer protein-lipid complex seems to be differentially segregated during the ACD, I speculate that the essential components of this protein-lipid complex are asymmetrically localized in highly polarized protodermal/epidermal cells. In chapter-IV, I especially focused on the interplay between plant cell polarity and sphingolipid metabolism.

I first observed the expression pattern of key enzymes for VLCFA-Cer synthesis. I showed that the expression of PAS2, an essential and rate-limiting enzyme for VLCFA synthesis (Bach et al., 2008) , was almost identical to that of ATML1 (Fig. IV-3, 4). Previous researches have also shown that only epidermal cells have abilities to synthesis VLCFAs in leaves (Sato, 1985) and that the expression patterns of various enzymes that are components of FAE are epidermis-specific (Joubes et al., 2008; Nobusawa et al., 2013) . Thus, the ATML1-expressing outermost cells are the primary sites for VLCFA synthesis.

該当部分に関して、5 年以内に雑誌で刊行予定のため、非公開。

Furthermore, I also found that the *de novo* expression of *PAS2* which likely plays a role in specific cell functions, such as suberin formation in the endodermis, is evoked in cells where *ATML1* is not expressed (Fig. IV-5). Collectively, a simultaneous inheritance of ATML1 and VLCFA-Cer or a simultaneous induction of the synthesis of ATML1 and VLCFA-Cer are suggested to be required for the maintenance or establishment of *ATML1* expression.

Finally, my results revealed that inhibition of the synthesis of VLCFA-sphingolipids affects apical membrane compartmentation (Fig. IV-8), suggesting the formation of a lipid-raft-rich apical membrane in plant epidermal cells, similar to mammalian epithelial cells (Simons and Ikonen, 1997; Surma et al., 2012). This is consistent with my idea that ceramides and complex sphingolipids which contain saturated VLCFAs, not unsaturated VLCFAs, are specific to the highly organized epidermal cell membrane, because the sphingolipids containing saturated VLCFAs rather than unsaturated VLCFAs are separated to a liquid-ordered state in which rafts likely exist (Kaiser et al., 2009).

Taken together, protodermal/epidermal cells have specific sphingolipid environment whose biophysical property facilitates a separation of the plasma membrane into distinct compartments. Such a lateral phase separation of sphingolipids in protodermal/epidermal cell membranes may have a key role in asymmetric segregation of the ATML1-VLCFA-Cer protein-lipid complex during the ACD.

It is still unclear how and where the ceramides as signaling molecules are generated and interact with ATML1. Importantly, complex sphingolipids are primarily located in the outer leaflet of plasma membrane in eukaryotic cells (Devaux and Morris, 2004). In mammalian cells, several ceramide species are generated as signaling molecules by hydrolysis of sphingomyelin in the outer leaflet and they interact with intracellular target molecules via trans-bilayer movement (Stancevic and Kolesnick, 2010). Therefore, in plant outermost cells, a sphingolipid hydrolase responsible for digesting the polar headgroups of VLCFA-sphingolipids is expected to be required for generation of VLCFA-Cers as signaling molecules (Fig. IV-9).

Furthermore, I hypothesized that VLCFA-Cers generated in the membrane is captured by ATML1 in the cytoplasm, because ATML1 is localized to the nuclei and cytoplasm (Iida et al., 2019) . Considering that the complete loss of GIPCs, not that of GluCers, results in the embryonic lethality (Msanne et al., 2015; Tartaglio et al., 2017; Jiang et al., 2019), GIPC-specific phospholipase C, which is predominantly located in the apical membrane of the outermost cells may be a good candidate for a key regulator in generating a ligand for ATML1 (Fig. IV-9).
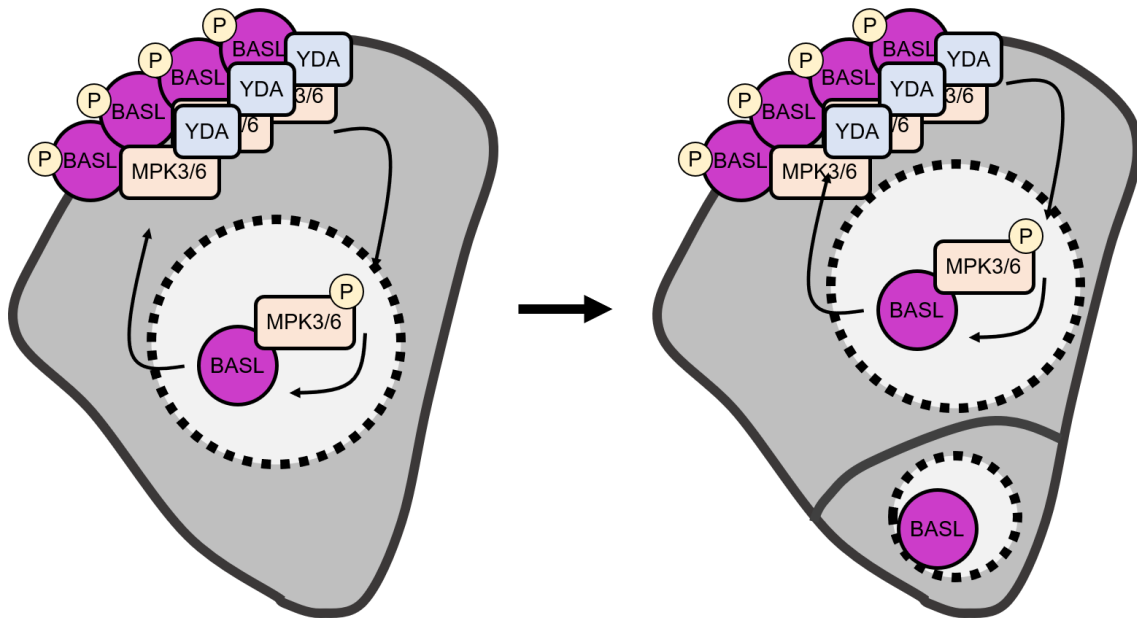
Fig. IV-1 Schematic representation of differential cell fate specification in stomatal ACD.

BASL and the YDA MAPK cascade constitute a feedback loop, and thus establish cell polarity including asymmetric MAPK activity in stomatal ACD precursor cells. Because MAPK activity directs SPCH levels, asymmetric MAPK activity in stomatal ACD precursor cells eventuates in differential cell fates between SLGCs and meristemoids.
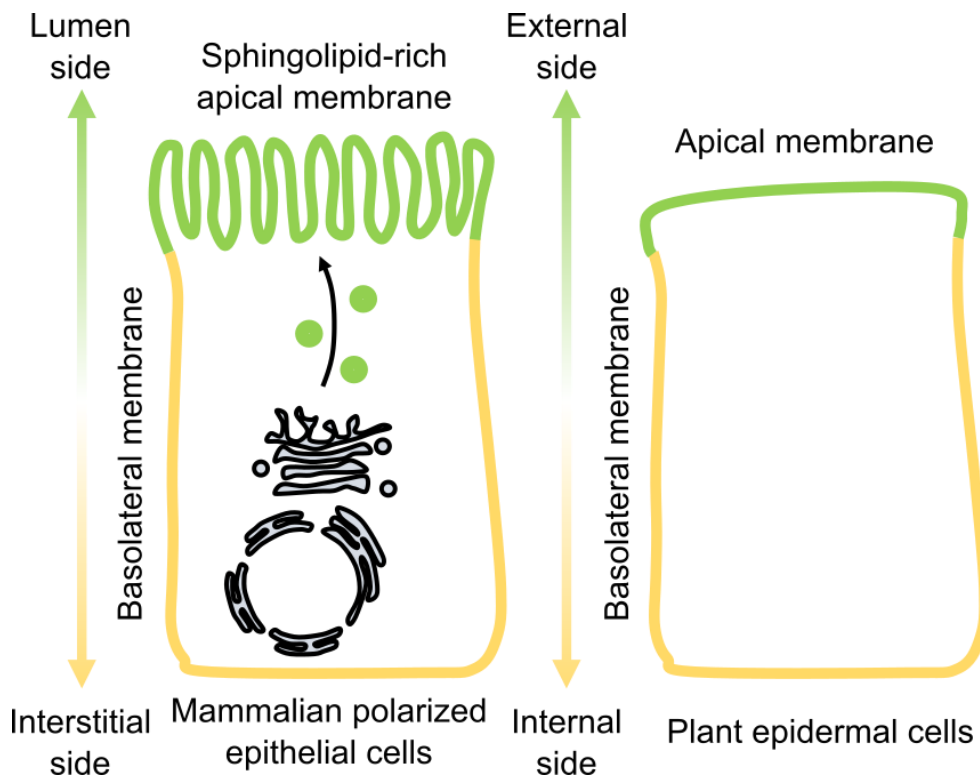
Fig. IV-2 Schematic representations of apical membrane compartmentation in mammalian epithelial cells and plant epidermal cells.

The plasma membranes of both mammalian epithelial cells and plant epidermal cells are highly organized into distinct apical and basolateral domains. In mammalian epithelial cells, two major plasma membrane bound pathways, apical and basolateral routes, originate from the trans-Golgi network (TGN). The apical route depends on lipid raft, whereas the basolateral route depends on various coats and their associated adaptor proteins. Lipid rafts-mediated trafficking to the apical membrane results in sphingolipid-rich apical membrane compartmentation. (Nagata et al., 2021)
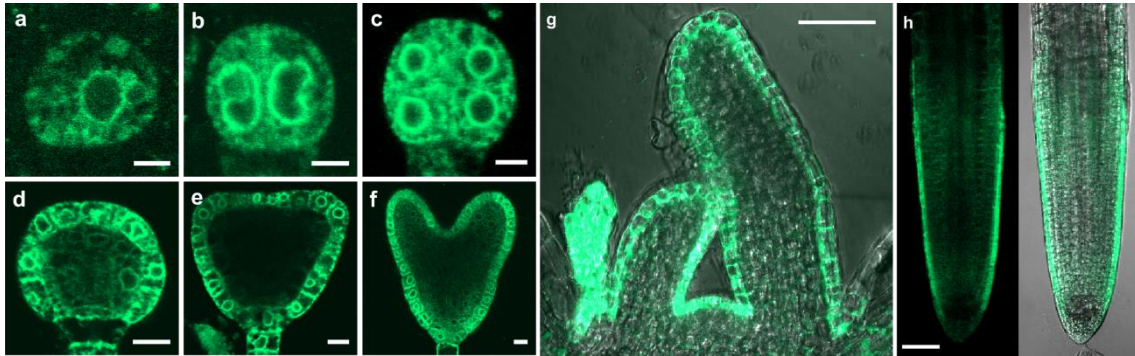
Fig. IV-3 *PAS2* expression pattern at various developmental stages.

(a), 1-cell stage embryo. **(b),** 2-cell stage embryo. **(c),** Octant stage embryo. **(d),**

Globular stage embryo. **(e),** Triangular stage embryo. **(f),** Torpedo stage embryo. **(g),**

Shoot apical meristem and leaf primordia. **(h),** Primary root before root-cap detachment.

Fluorescence image (left) and merged fluorescence and bright field image (right). Scale

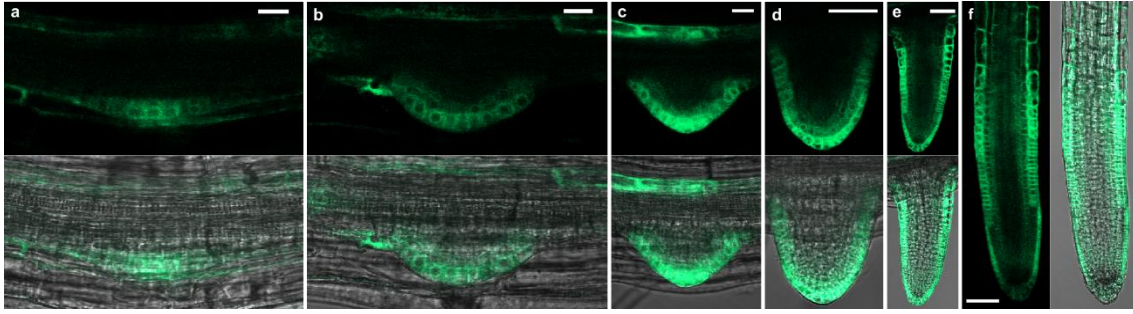bars: 5µm in (a-c); 10 µm in (d-f); 50 µm in (g, h). (Nagata et al., 2021)

Fig. IV-4 *PAS2* expression pattern during LR development.

(a), Stage-II lateral root primordia(LRPs). **(b),** Stage-III/IV LRP. **(c),** Stage-VI LRP. **(d),** Emerged lateral root. **(e),** Elongated lateral root. In **(a-e)**, the fluorescence images are shown in the top panels, and the merged fluorescence and bright field images are shown in the bottom panels. **(f),** Lateral root before root-cap detachment. Fluorescence image (left) and merged fluorescence and bright field image (right). Scale bars: 20 μm in (a-c); 50 μm in (d, e, f). (Nagata et al., 2021)

該当部分に関して、5 年以内に雑誌で刊行予定のため、非公開。

該当部分に関して、5 年以内に雑誌で刊行予定のため、非公開。

該当部分に関して、5 年以内に雑誌で刊行予定のため、非公開。
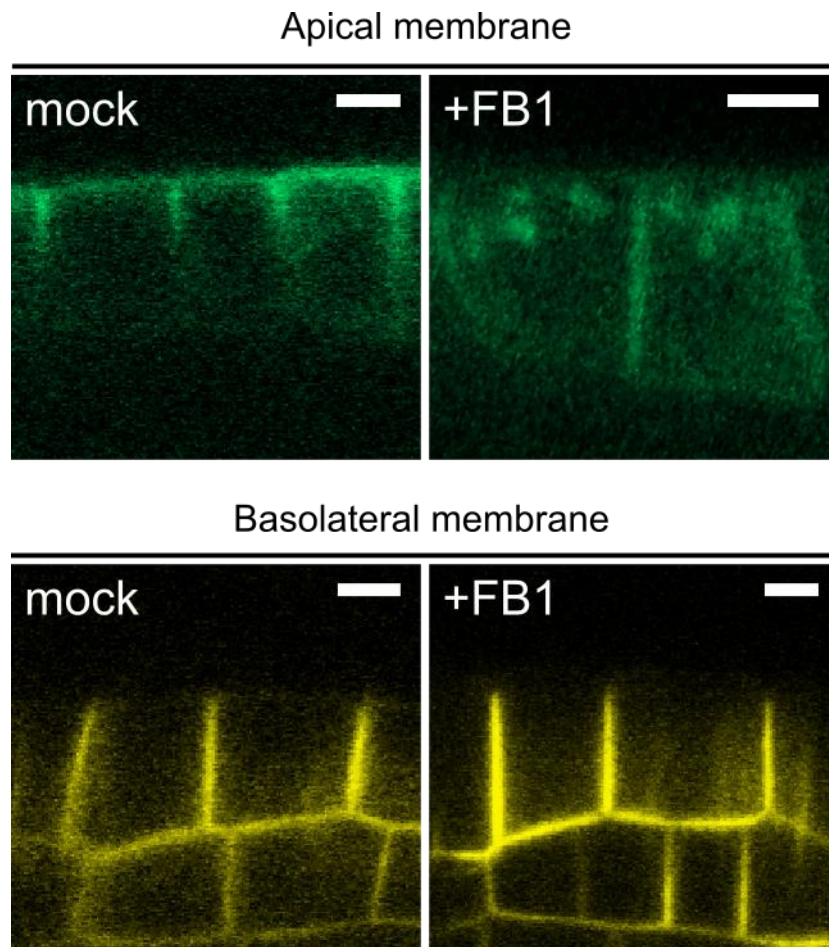
該当部分に関して、5 年以内に雑誌で刊行予定のため、非公開。

Fig. IV-8 Subcellular localization of apical or basolateral membrane specific proteins with mock or 3 μM FB1 treatment.

Fluorescence images of EGFP-WBC11 in the outermost cells with mock (top-left) or short-term 3 μM FB1 (top-right) treatment and that of YFP-REM1.2 in the outermost cells with mock (bottom-left) or short-term 3 μM FB1 (bottom-right) treatment. Scale bars: 5μm. (Nagata et al., 2021)
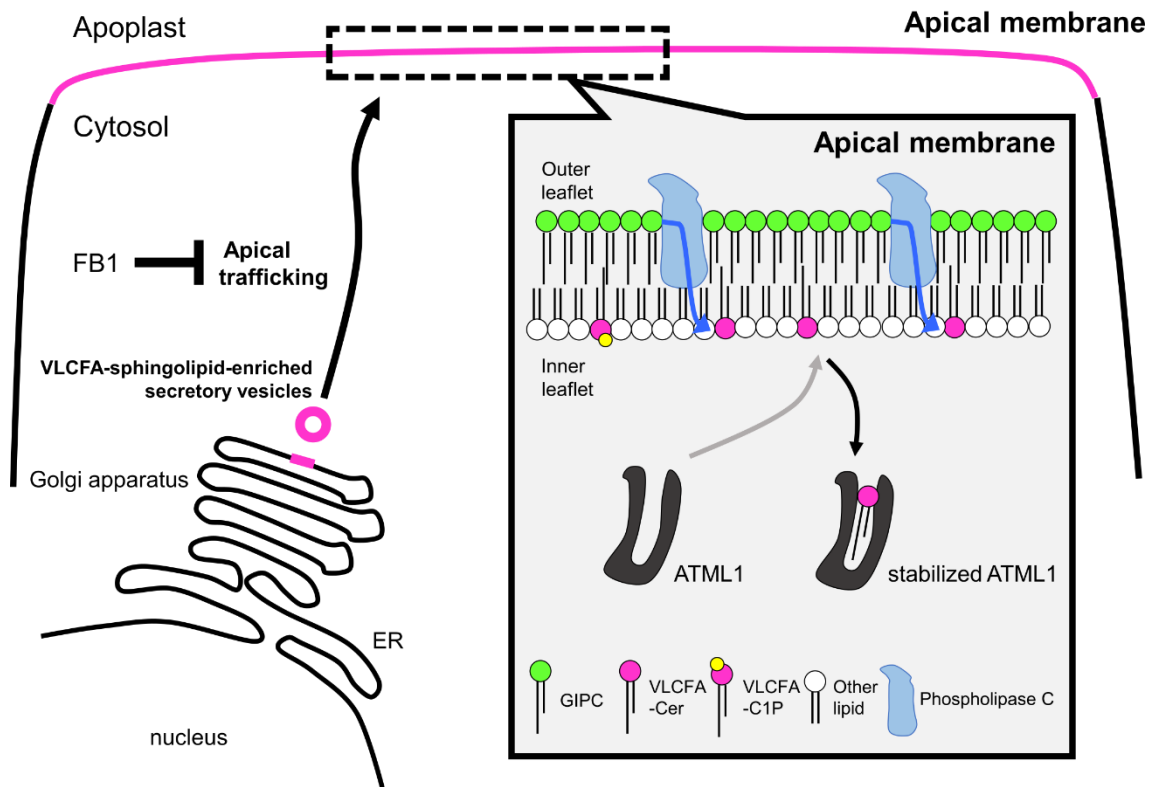
Fig. IV-9 Schematic model of VLCFA-Cer generation in the apical membrane of epidermal cells.

Trafficking of VLCFA-sphingolipids to the apical membrane and generation of VLCFA-Cers, which interact with intracellular ATML1. VLCFA-sphingolipids are transported to the apical membrane by a mechanism that is inhibited by FB1 treatment. Subsequently, VLCFA-sphingolipids (such as GIPCs) in the outer leaflet of the apical membrane are hydrolyzed by specific enzymes (such as Phospholipase C), generating VLCFA-Cers in the inner leaflet of the apical membrane. The magenta line indicates apical membrane components. ER, endoplasmic reticulum. (Nagata et al., 2021)

Chapter-V

General Discussion

All vascular plants are organized into three fundamental tissue systems: the epidermis, the ground tissue and the vascular tissue (Goldberg et al., 1994; Jurgens, 1995). The arrangement of each tissue is highly coordinated along a body axis, representing the robustness in the plant development. In contrast, plants can adapt to and cope with fluctuations in the external environment by altering their physiologies and/or morphologies. This ability represents the plasticity in the plant development and is especially required for plants rather than animals owing to their sessile lifestyle. Because the molecular basis underlying the phenotypic plasticity and robustness are not fully different but found on dynamic interplay among a number of common factors, it is important to elucidate the fundamental regulatory mechanism of key genes for understanding the excellence of plant lifestyle from the molecular genetic perspective.

Here, I have provided an initial characterization of VLCFA-Cers-mediated positional signaling in Arabidopsis. My analysis revealed that ATML1 protein allocated to the inner cells through ACDs of epidermal cells or by a misexpression soon disappeared from the inner cells. I also found that stabilization of the ATML1 protein is dependent on the interaction with VLCFA-Cers and that the interaction between ATML1 and VLCFA-Cers is crucial for the function of ATML1 in the outermost cells. Therefore,

VLCFA-Cers are considered as an essential component of cell position- and cell lineage-dependent positional signaling in Arabidopsis.

In plants, the idea that relative cell position rather than absolute cell lineage plays a crucial role in the acquisition of cell identity is widely accepted (Stewart and Dermen, 1975; van den Berg et al., 1995; Scheres, 2001; Leyser and Day, 2009). However, the determination of the relative position requires absolute reference especially when the robustness is necessitated. For instance, the generation of "inner" cells ultimately require the presence of the outermost cells. Subsequently, the cells with two distinct positions could establish the radial axis of plant body. Thereafter, "outer" cell position and "inner" cell position could be recognized by a variety of inner cells according to the radial body axis, realizing cell-position-dependent fate determination of inner cells. Thus, the establishment of the relative-cell-position-dependent construction of a complicated inner structure firstly requires the presence of the outermost cell layer as an absolute reference. Consistently, it is known that the cells which compose the early embryos including the zygote exhibit the epidermal cell properties such as a cuticle formation (Bruck and Walker, 1985; Lu et al., 1996; Takada and Jurgens, 2007).

One of the remaining questions is when and how the expression of ATML1/PDF2 and VLCFA-Cer synthesis-related genes is firstly established, because

the germline cells of plants are initiated from subepidermal cells (Zhou et al., 2017) and

the lateral root is initiated from the pericycle cells (Malamy and Benfey, 1997). Auxin

may be a good candidate for the inducer of the *de novo* establishment of the expressions

of ATML1/PDF2 and VLCFA-Cer-synthesis-related genes. Several auxin response

elements (AuxRE; Ulmasov et al., 1995; Hagen and Guilfoyle, 2002; Guilfoyle and

Hagen, 2007; Chapman and Estelle, 2009) are found in the upstream region from the

putative transcription start site of *ATML1* (TGTCCC at -485bp, and TGTCAC at -420bp

and -1276bp) and *PDF2* (TGTCTC at -1972bp and -2047bp, and TGTCAC at -

1614bp). In addition, a recent study shows that the AP2 family auxin-inducible TF

PUCHI induces multiple genes coding for VLCFA biosynthesis enzymes during lateral

root and callus formation (Trinh et al., 2019). Besides, as GIPCs are suggested to be

present in pollen grain (Rennie et al., 2014; Tartaglio et al., 2017), it is also conceivable

that specific sphingolipids are transmitted from germ cells to the zygotes.

However, in this context, auxin-induced *de novo* expression of *ATML1* and

PDF2 in the differentiated tissue must be strictly restricted. A repressive epigenetic

modification to the Histone H3 (H3K27me3) accumulated in the promoters of *ATML1*

and *PDF2* may play a key role in the repression of the auxin-mediated induction of

these genes in the differentiated cells (Fig. V-1).

Altogether, I propose a working model regarding the molecular determination of outermost and inner cells (Fig. V-2). Apical membrane components of the outermost cells are neither passed on to inner-daughter cells through periclinal divisions nor to outermost cells derived from inner lineages. The membrane of the zygote is composed of only apical membrane. In addition, the membrane of the pericycle cells, which initiates lateral root primordium, are highly polarized (Friml et al., 2002; Blilou et al., 2005), similar to that of the epidermal cells. Therefore, apical membrane components of these cells are inherited asymmetrically to their daughter cells though ACDs and thus could serve as an essential component in establishing and maintaining the radial-axis in cooperation with the key TFs in epidermis differentiation in plants.

Nevertheless, previous researches demonstrated that ectopic over-expression of ATML1 from constitutive promoter can induce the formation of outermost-specific cell types, such as stomatal cells and trichome-like cells even in the inner cell position (Peterson et al., 2013; Takada et al., 2013). Although the patchy induction pattern of the formation of cells similar to the epidermal cells in inner position suggests that inner cell position does not fully empower the activity of ectopically induced ATML1 proteins, these observations seem to be a clear counterexample of the proposed model in this study.

CERT, a mammalian START-containing protein that are firstly identified as an intermembrane transfer protein of C16-ceramide in *vivo* (Hanada et al., 2003), can transfer various types of ceramides and even diacylglycerol in *vitro*, although the transfer efficiency of some of them were much lower than that of the C16-ceramide (Kumagai et al., 2005). Furthermore, artificial TFs carrying various START domains from mammals and plants bind to a number of small metabolites in yeast (Schrick et al., 2014). These results suggest that START domain is able to bind to an unnatural ligand and partially exert its biological function. Consistently, I found that START domain of ATML1 can bind a variety of lipid species. It is conceivable that constitutively overexpressed ATML1 proteins form the unusual protein-lipid complexes with low TF abilities and the amount of them exceeds a threshold concentration required for the induction of epidermis-related gene by chance, resulting in patchy formation of epidermis-related tissues in inner cell position.

Adaptation to a terrestrial lifestyle has necessitated the evolution of a basic body plan that can achieve epidermis differentiation at appropriate positions. Remarkably, the START domains in plants are primarily found within homeodomain TFs, comprising the HD-START family that orchestrates various morphogenetic processes to build up a three dimensional plant multicellular body compatible with

terrestrial life (Schrick et al., 2004). The HD-START family is confined to the plant

kingdom, implying that the association between organism specific lipids and the HD-

START family represents an inevitable evolutionary strategy for sessile plants.

ATML1
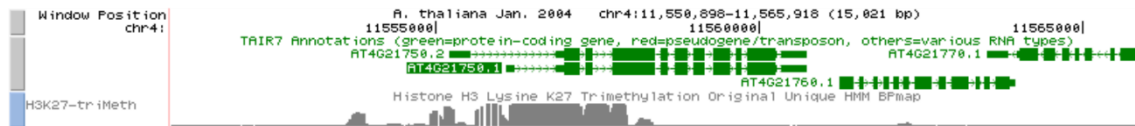
PDF2
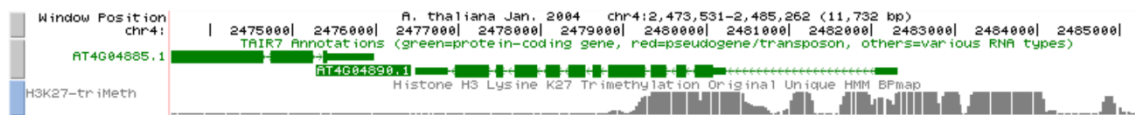

Fig. V-1 H3K27me3 accumulation in the promoters of ATML1 and PDF2 .

UCSC Genome Browser (http://epigenomics.mcdb.ucla.edu/H3K27m3/) output

showing the accumulation of H3K27me3 in the promoters of ATML1(top panel) and
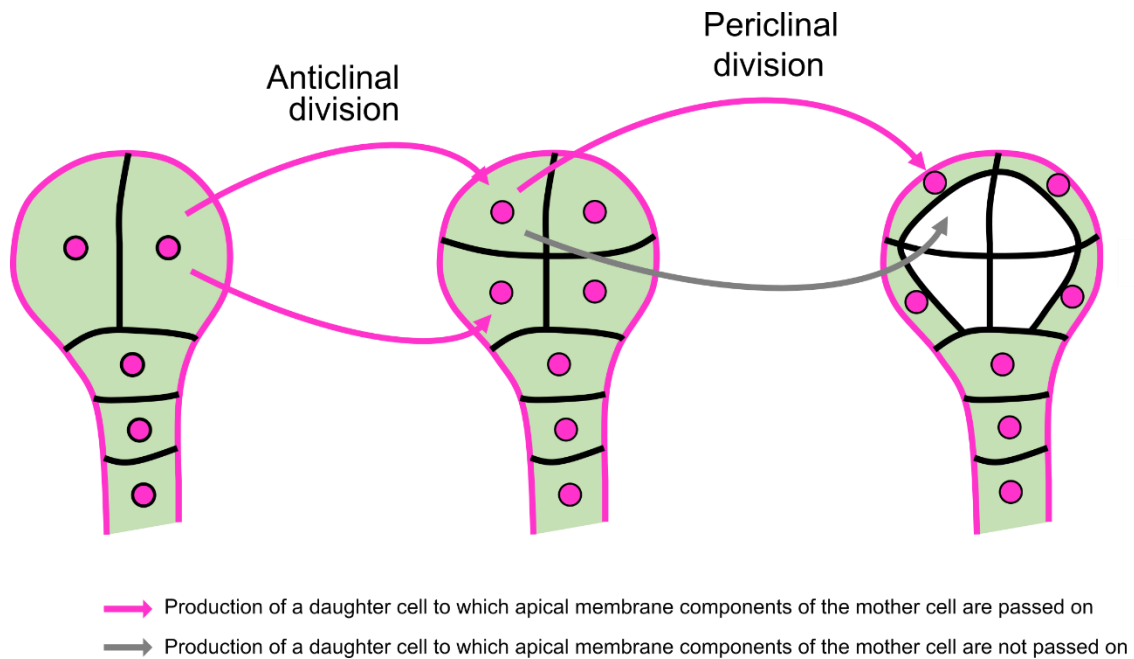
PDF2(bottom panel).

Fig.V-2 Schematic model of the molecular determination of the outermost and inner cells.

Location of ATML1 expression and the apical membrane which is passed on to daughter cells from a mother cell in the outermost position. 4-cell stage embryo (left), octant stage embryo (middle) and dermatogen stage embryo (right) are shown as representative examples. Anticlinal division of an outermost cell generates two outermost daughter cells with apical membranes. Periclinal division of an outermost cell generates one outermost daughter cell with apical membrane and one inner daughter cell without apical membrane. The magenta circle indicates *ATML1* expression. The magenta line indicates the apical membranes of outermost cells.

References

Abe, M., Katsumata, H., Komeda, Y. and Takahashi, T. (2003). Regulation of Shoot Epidermal Cell Differentiation by a Pair of Homeodomain Proteins in Arabidopsis. *Development* **130,** 635-643.

Abe, M., Takahashi, T. and Komeda, Y. (2001). Identification of a Cis-Regulatory Element for L1 Layer-Specific Gene Expression, which is Targeted by an L1-Specific Homeodomain Protein. *Plant J.* **26,** 487-494.

Bach, L., Michaelson, L. V., Haslam, R., Bellec, Y., Gissot, L., Marion, J., Da Costa, M., Boutin, J. P., Miquel, M., Tellier, F. et al. (2008). The very-Long-Chain Hydroxy Fatty Acyl-CoA Dehydratase PASTICCINO2 is Essential and Limiting for Plant Development. *Proc. Natl. Acad. Sci. U. S. A.* **105,** 14727-14731.

Beaudoin, F., Wu, X., Li, F., Haslam, R. P., Markham, J. E., Zheng, H., Napier, J. A. and Kunst, L. (2009). Functional Characterization of the Arabidopsis Beta-Ketoacyl-Coenzyme A Reductase Candidates of the Fatty Acid Elongase. *Plant Physiol.* **150,** 1174-1191.

Berkey, R., Bendigeri, D. and Xiao, S. (2012). Sphingolipids and Plant Defense/Disease: The "Death" Connection and Beyond. *Front. Plant. Sci.* **3,** 68.

Blilou, I., Xu, J., Wildwater, M., Willemsen, V., Paponov, I., Friml, J., Heidstra, R., Aida, M., Palme, K. and Scheres, B. (2005). The PIN Auxin Efflux Facilitator Network Controls Growth and Patterning in Arabidopsis Roots. *Nature* **433,** 39.

Bruck, D. K. and Walker, D. B. (1985). Cell Determination during Embryogenesis in Citrus Jambhiri. I. Ontogeny of the Epidermis. *Botanical Gazette* **146,** 188-195.

Cacas, J. L., Bure, C., Grosjean, K., Gerbeau-Pissot, P., Lherminier, J., Rombouts, Y., Maes, E., Bossard, C., Gronnier, J., Furt, F. et al. (2016). Revisiting Plant Plasma Membrane Lipids in Tobacco: A Focus on Sphingolipids. *Plant Physiol.* **170,** 367-384.

Chapman, E. J. and Estelle, M. (2009). Mechanism of Auxin-Regulated Gene Expression in Plants. *Annu. Rev. Genet.* **43,** 265-285.

Clark, B. J., Wells, J., King, S. R. and Stocco, D. M. (1994). The Purification, Cloning, and Expression of a Novel Luteinizing Hormone-Induced Mitochondrial Protein in MA-10 Mouse Leydig Tumor Cells. Characterization of the Steroidogenic Acute Regulatory Protein (StAR). *J. Biol. Chem.* **269,** 28314-28322.

Clough, S. J. and Bent, A. F. (1998). Floral Dip: A Simplified Method for Agrobacterium-Mediated Transformation of Arabidopsis thaliana. *Plant J.* **16,** 735-743.

Devaux, P. F. and Morris, R. (2004). Transmembrane Asymmetry and Lateral Domains in Biological Membranes. *Traffic* **5,** 241-246.

Dong, J., MacAlister, C. A. and Bergmann, D. C. (2009). BASL Controls Asymmetric Cell Division in Arabidopsis. *Cell* **137,** 1320-1330.

Dowler, S., Kular, G. and Alessi, D. R. (2002). Protein Lipid Overlay Assay. *Sci.STKE* **2002,** pl6.

Friml, J., Wiśniewska, J., Benková, E., Mendgen, K. and Palme, K. (2002). Lateral Relocation of Auxin Efflux Regulator PIN3 Mediates Tropism in Arabidopsis. *Nature* **415,** 806.

Galletti, R., Verger, S., Hamant, O. and Ingram, G. C. (2016). Developing a 'Thick Skin': A Paradoxical Role for Mechanical Tension in Maintaining Epidermal Integrity? *Development* **143,** 3249-3258.

Gifford, M. L., Dean, S. and Ingram, G. C. (2003). The Arabidopsis ACR4 Gene Plays a Role in Cell Layer Organisation during Ovule Integument and Sepal Margin Development. *Development* **130,** 4249-4258.

Goldberg, R. B., de Paiva, G. and Yadegari, R. (1994). Plant Embryogenesis: Zygote to Seed. *Science* **266,** 605-614.

Guilfoyle, T. J. and Hagen, G. (2007). Auxin Response Factors. *Curr. Opin. Plant Biol.* **10,** 453-460.

Hagen, G. and Guilfoyle, T. (2002). Auxin-Responsive Gene Expression: Genes, Promoters and Regulatory Factors. *Plant Mol. Biol.* **49,** 373-385.

Hanada, K., Kumagai, K., Yasuda, S., Miura, Y., Kawano, M., Fukasawa, M. and Nishijima, M. (2003). Molecular Machinery for Non-Vesicular Trafficking of Ceramide. *Nature* **426,** 803-809.

Iida, H., Yoshida, A. and Takada, S. (2019). ATML1 Activity is Restricted to the Outermost Cells of the Embryo through Post-Transcriptional Repressions. *Development* **146,** 10.1242/dev.169300.

Ishikawa, T., Aki, T., Yanagisawa, S., Uchimiya, H. and Kawai-Yamada, M. (2015). Overexpression of BAX INHIBITOR-1 Links Plasma Membrane Microdomain Proteins to Stress. *Plant Physiol.* **169,** 1333-1343.

Ishikawa, T., Fang, L., Rennie, E. A., Sechet, J., Yan, J., Jing, B., Moore, W., Cahoon, E. B., Scheller, H. V. and Kawai-Yamada, M. (2018). GLUCOSAMINE INOSITOLPHOSPHORYLCERAMIDE TRANSFERASE1 (GINT1) is a GlcNAc-Containing Glycosylinositol Phosphorylceramide Glycosyltransferase. *Plant Physiol.* **177,** 938-952.

Ishikawa, T., Ito, Y. and Kawai‐Yamada, M. (2016). Molecular Characterization and Targeted Quantitative Profiling of the Sphingolipidome in Rice. *Plant J.* **88,** 681-693.

Jarsch, I. K., Konrad, S. S., Stratil, T. F., Urbanus, S. L., Szymanski, W., Braun, P., Braun, K. and Ott, T. (2014). Plasma Membranes are Subcompartmentalized into a Plethora of Coexisting and Diverse Microdomains in Arabidopsis and *Nicotiana benthamiana*. *Plant Cell* **26,** 1698-1711.

Jiang, Z., Zhou, X., Tao, M., Yuan, F., Liu, L., Wu, F., Wu, X., Xiang, Y., Niu, Y., Liu, F. et al. (2019). Plant Cell-Surface GIPC Sphingolipids Sense Salt to Trigger Ca(2+) Influx. *Nature* **572,** 341-346.

Joubes, J., Raffaele, S., Bourdenx, B., Garcia, C., Laroche-Traineau, J., Moreau, P., Domergue, F. and Lessire, R. (2008). The VLCFA Elongase Gene Family in *Arabidopsis thaliana*: Phylogenetic Analysis, 3D Modelling and Expression Profiling. *Plant Mol. Biol.* **67,** 547-566.

Jurgens, G. (1995). Axis Formation in Plant Embryogenesis: Cues and Clues. *Cell* **81,** 467-470.

Kaiser, H. J., Lingwood, D., Levental, I., Sampaio, J. L., Kalvodova, L., Rajendran, L. and Simons, K. (2009). Order of Lipid Phases in Model and Plasma Membranes. *Proc. Natl. Acad. Sci. U. S. A.* **106,** 16645-16650.

Kitatani, K., Idkowiak-Baldys, J. and Hannun, Y. A. (2008). The Sphingolipid Salvage Pathway in Ceramide Metabolism and Signaling. *Cell. Signal.* **20,** 1010-1018.

Kumagai, K., Yasuda, S., Okemoto, K., Nishijima, M., Kobayashi, S. and Hanada, K. (2005). CERT Mediates Intermembrane Transfer of various Molecular Species of Ceramides. *J. Biol. Chem.* **280,** 6488-6495.

Kumpf, R. P. and Nowack, M. K. (2015). The Root Cap: A Short Story of Life and Death. *J. Exp. Bot.* **66,** 5651-5662.

Leyser, O. and Day, S. (2009). *Mechanisms in Plant Development*: John Wiley & Sons.

Li-Beisson, Y., Shorrosh, B., Beisson, F., Andersson, M. X., Arondel, V., Bates, P. D., Baud, S., Bird, D., Debono, A., Durrett, T. P. et al. (2013). Acyl-Lipid Metabolism. *Arabidopsis Book* **11,** e0161.

Lu, P., Porat, R., Nadeau, J. A. and O'Neill, S. D. (1996). Identification of a Meristem L1 Layer-Specific Gene in Arabidopsis that is Expressed during Embryonic Pattern Formation and Defines a New Class of Homeobox Genes. *Plant Cell* **8,** 2155-2168.

Luo, B., Xue, X., Hu, W., Wang, L. and Chen, X. (2007). An ABC Transporter Gene of Arabidopsis Thaliana, AtWBC11, is Involved in Cuticle Development and Prevention of Organ Fusion. *Plant Cell Physiol.* **48,** 1790-1802.

Luttgeharm, K. D., Cahoon, E. B. and Markham, J. E. (2016). Substrate Specificity, Kinetic Properties and Inhibition by Fumonisin B1 of Ceramide Synthase Isoforms from Arabidopsis. *Biochem. J.* **473,** 593-603.

Lv, X., Jing, Y., Xiao, J., Zhang, Y., Zhu, Y., Julian, R. and Lin, J. (2017). Membrane Microdomains and the Cytoskeleton Constrain AtHIR1 Dynamics and Facilitate the Formation of an AtHIR1-Associated Immune Complex. *Plant J.* **90,** 3-16.

Malamy, J. E. and Benfey, P. N. (1997). Organization and Cell Differentiation in Lateral Roots of *Arabidopsis thaliana*. *Development* **124,** 33-44.

Markham, J. E., Molino, D., Gissot, L., Bellec, Y., Hematy, K., Marion, J., Belcram, K., Palauqui, J. C., Satiat-Jeunemaitre, B. and Faure, J. D. (2011). Sphingolipids Containing very-Long-Chain Fatty Acids Define a Secretory Pathway for Specific Polar Plasma Membrane Protein Targeting in Arabidopsis. *Plant Cell* **23,** 2362-2378.

Merrill Jr, A. H. (2011). Sphingolipid and Glycosphingolipid Metabolic Pathways in the Era of Sphingolipidomics. *Chem. Rev.* **111,** 6387-6422.

Morell, M., Espargaro, A., Aviles, F. X. and Ventura, S. (2007). Detection of Transient Protein-Protein Interactions by Bimolecular Fluorescence Complementation: The Abl-SH3 Case. *Proteomics* **7,** 1023-1036.

Msanne, J., Chen, M., Luttgeharm, K. D., Bradley, A. M., Mays, E. S., Paper, J. M., Boyle, D. L., Cahoon, R. E., Schrick, K. and Cahoon, E. B. (2015). Glucosylceramides are Critical for Cell-Type Differentiation and Organogenesis, but Not for Cell Viability in Arabidopsis. *Plant J.* **84,** 188-201.

Murashige, T. and Skoog, F. (1962). A Revised Medium for Rapid Growth and Bio Assays with Tobacco Tissue Cultures. *Physiol. Plantarum* **15,** 473-497.

Nagano, M., Ishikawa, T., Fujiwara, M., Fukao, Y., Kawano, Y., Kawai-Yamada, M. and Shimamoto, K. (2016). Plasma Membrane Microdomains are Essential for Rac1-RbohB/H-Mediated Immunity in Rice. *Plant Cell* **28,** 1966-1983.

Nakamura, M. and Grebe, M. (2018). Outer, Inner and Planar Polarity in the Arabidopsis Root. *Curr. Opin. Plant Biol.* **41,** 46-53.

Nobusawa, T., Okushima, Y., Nagata, N., Kojima, M., Sakakibara, H. and Umeda, M. (2013). Synthesis of very-Long-Chain Fatty Acids in the Epidermis Controls Plant Organ Growth by Restricting Cell Proliferation. *PLoS Biol.* **11,** e1001531.

Nobusawa, T. and Umeda, M. (2012). Very-Long-Chain Fatty Acids have an Essential Role in Plastid Division by Controlling Z-Ring Formation in *Arabidopsis thaliana*. *Genes Cells* **17,** 709-719.

Ogawa, E., Yamada, Y., Sezaki, N., Kosaka, S., Kondo, H., Kamata, N., Abe, M., Komeda, Y. and Takahashi, T. (2015). ATML1 and PDF2 Play a Redundant and Essential Role in Arabidopsis Embryo Development. *Plant Cell Physiol.* **56,** 1183-1192.

Panikashvili, D. and Aharoni, A. (2008). ABC-Type Transporters and Cuticle Assembly: Linking Function to Polarity in Epidermis Cells. *Plant. Signal. Behav.* **3,** 806-809.

Pata, M. O., Hannun, Y. A. and Ng, C. K. (2010). Plant Sphingolipids: Decoding the Enigma of the Sphinx. *New Phytol.* **185,** 611-630.

Peterson, K. M., Shyu, C., Burr, C. A., Horst, R. J., Kanaoka, M. M., Omae, M., Sato, Y. and Torii, K. U. (2013). Arabidopsis Homeodomain-Leucine Zipper IV Proteins Promote Stomatal Development and Ectopically Induce Stomata Beyond the Epidermis. *Development* **140,** 1924-1935.

Rennie, E. A., Ebert, B., Miles, G. P., Cahoon, R. E., Christiansen, K. M., Stonebloom, S., Khatab, H., Twell, D., Petzold, C. J., Adams, P. D. et al. (2014). Identification of a Sphingolipid Alpha-Glucuronosyltransferase that is Essential for Pollen Function in Arabidopsis. *Plant Cell* **26,** 3314-3325.

Rombola-Caldentey, B., Rueda-Romero, P., Iglesias-Fernandez, R., Carbonero, P. and Onate-Sanchez, L. (2014). Arabidopsis DELLA and Two HD-ZIP Transcription Factors Regulate GA Signaling in the Epidermis through the L1 Box Cis-Element. *Plant Cell* **26,** 2905-2919.

Sato, N. (1985). Lipid Biosynthesis in Epidermal, Guard and Mesophyll Cell Protoplasts from Leaves of Vicia Faba L. *Plant Cell physiol.* **26,** 805-811.

Scheres, B. (2001). Plant Cell Identity. the Role of Position and Lineage. *Plant Physiol.* **125,** 112-114.

Scheres, B., Wolkenfelt, H., Willemsen, V., Terlouw, M., Lawson, E., Dean, C. and Weisbeek, P. (1994). Embryonic Origin of the Arabidopsis Primary Root and Root Meristem Initials. *Development* **120,** 2475-2487.

Schmidt, A. (1924). Histologische Studien an Phanerogamen Vegetationspunkten. *Bot.Arch.* **8,** 345-404.

Schrick, K., Bruno, M., Khosla, A., Cox, P. N., Marlatt, S. A., Roque, R. A., Nguyen, H. C., He, C., Snyder, M. P., Singh, D. et al. (2014). Shared Functions of Plant and Mammalian StAR-Related Lipid Transfer (START) Domains in Modulating Transcription Factor Activity. *BMC Biol.* **12,** 70-8.

Schrick, K., Nguyen, D., Karlowski, W. M. and Mayer, K. F. (2004). START Lipid/Sterol-Binding Domains are Amplified in Plants and are Predominantly Associated with Homeodomain Transcription Factors. *Genome Biol.* **5,** R41-r41. Epub 2004 May 27.

Sessions, A., Weigel, D. and Yanofsky, M. F. (1999). The *Arabidopsis thaliana* MERISTEM LAYER 1 Promoter Specifies Epidermal Expression in Meristems and Young Primordia. *Plant J.* **20,** 259-263.

Silva, L. C., Futerman, A. H. and Prieto, M. (2009). Lipid Raft Composition Modulates Sphingomyelinase Activity and Ceramide-Induced Membrane Physical Alterations. *Biophys. J.* **96,** 3210-3222.

Simons, K. and Ikonen, E. (1997). Functional Rafts in Cell Membranes. *Nature* **387,** 569.

Stancevic, B. and Kolesnick, R. (2010). Ceramide-Rich Platforms in Transmembrane Signaling. *FEBS Lett.* **584,** 1728-1740.

Steiner, D. F. (1998). The Proprotein Convertases. *Curr. Opin. Chem. Biol.* **2,** 31-39.

Stewart, R. N. and Dermen, H. (1975). Flexibility in Ontogeny as shown by the Contribution of the Shoot Apical Layers to Leaves of Periclinal Chimeras. *Am. J. Bot.* **62,** 935-947.

Surma, M. A., Klose, C. and Simons, K. (2012). Lipid-Dependent Protein Sorting at the Trans-Golgi Network. *Biochim. Biophys. Acta* **1821,** 1059-1067.

Takada, S. and Jurgens, G. (2007). Transcriptional Regulation of Epidermal Cell Fate in the Arabidopsis Embryo. *Development* **134,** 1141-1150.

Takada, S., Takada, N. and Yoshida, A. (2013). Induction of Epidermal Cell Fate in Arabidopsis Shoots. *Plant. Signal. Behav.* **8,** e26236.

Takahashi, T., Naito, S. and Komeda, Y. (1992). The Arabidopsis HSP18. 2 Promoter/GUS Gene Fusion in Transgenic Arabidopsis Plants: A Powerful Tool for the Isolation of Regulatory Mutants of the Heat‐shock Response. *Plant J.* **2,** 751-761.

Tanaka, H., Onouchi, H., Kondo, M., Hara-Nishimura, I., Nishimura, M., Machida, C. and Machida, Y. (2001). A Subtilisin-Like Serine Protease is Required for Epidermal Surface Formation in Arabidopsis Embryos and Juvenile Plants. *Development* **128,** 4681-4689.

Tanaka, H., Watanabe, M., Sasabe, M., Hiroe, T., Tanaka, T., Tsukaya, H., Ikezaki, M., Machida, C. and Machida, Y. (2007). Novel Receptor-Like Kinase ALE2 Controls Shoot Development by Specifying Epidermis in Arabidopsis. *Development* **134,** 1643-1652.

Tartaglio, V., Rennie, E. A., Cahoon, R., Wang, G., Baidoo, E., Mortimer, J. C., Cahoon, E. B. and Scheller, H. V. (2017). Glycosylation of Inositol Phosphorylceramide Sphingolipids is Required for Normal Growth and Reproduction in Arabidopsis. *Plant J.* **89,** 278-290.

Terakura, S., Ueno, Y., Tagami, H., Kitakura, S., Machida, C., Wabiko, H., Aiba, H., Otten, L., Tsukagoshi, H., Nakamura, K. et al. (2007). An Oncoprotein from the Plant Pathogen Agrobacterium has Histone Chaperone-Like Activity. *Plant Cell* **19,** 2855-2865.

Trenkamp, S., Martin, W. and Tietjen, K. (2004). Specific and Differential Inhibition of very-Long-Chain Fatty Acid Elongases from *Arabidopsis thaliana* by Different Herbicides. *Proc. Natl. Acad. Sci. U. S. A.* **101,** 11903-11908.

Trinh, D. C., Lavenus, J., Goh, T., Boutte, Y., Drogue, Q., Vaissayre, V., Tellier, F., Lucas, M., Voss, U., Gantet, P. et al. (2019). PUCHI Regulates Very Long Chain Fatty Acid Biosynthesis during Lateral Root and Callus Formation. *Proc. Natl. Acad. Sci. U. S. A.* **116,** 14325-14330.

Tsuwamoto, R., Fukuoka, H. and Takahata, Y. (2008). GASSHO1 and GASSHO2 Encoding a Putative Leucine‐rich Repeat Transmembrane‐type Receptor Kinase are Essential for the Normal Development of the Epidermal Surface in Arabidopsis Embryos. *Plant J.* **54,** 30-42.

Ulmasov, T., Liu, Z. B., Hagen, G. and Guilfoyle, T. J. (1995). Composite Structure of Auxin Response Elements. *Plant Cell* **7,** 1611-1623.

van den Berg, C., Willemsen, V., Hage, W., Weisbeek, P. and Scheres, B. (1995). Cell Fate in the Arabidopsis Root Meristem Determined by Directional Signalling. *Nature* **378,** 62.

Watanabe, M., Tanaka, H., Watanabe, D., Machida, C. and Machida, Y. (2004). The ACR4 Receptor-Like Kinase is Required for Surface Formation of Epidermis-Related Tissues in *Arabidopsis thaliana*. *Plant J.* **39,** 298-308.

Xing, Q., Creff, A., Waters, A., Tanaka, H., Goodrich, J. and Ingram, G. C. (2013). ZHOUPI Controls Embryonic Cuticle Formation Via a Signalling Pathway Involving the Subtilisin Protease ABNORMAL LEAF-SHAPE1 and the Receptor Kinases GASSHO1 and GASSHO2. *Development* **140,** 770-779.

Yang, S., Johnston, N., Talideh, E., Mitchell, S., Jeffree, C., Goodrich, J. and Ingram, G. (2008). The Endosperm-Specific ZHOUPI Gene of Arabidopsis Thaliana Regulates Endosperm Breakdown and Embryonic Epidermal Development. *Development* **135,** 3501-3509.

Zhang, Y., Guo, X. and Dong, J. (2016). Phosphorylation of the Polarity Protein BASL Differentiates Asymmetric Cell Fate through MAPKs and SPCH. *Current Biology* **26,** 2957-2965.

Zhang, Y., Wang, P., Shao, W., Zhu, J. and Dong, J. (2015). The BASL Polarity Protein Controls a MAPK Signaling Feedback Loop in Asymmetric Cell Division. *Developmental Cell* **33,** 136-149.

Zhou, L. Z., Juranic, M. and Dresselhaus, T. (2017). Germline Development and Fertilization Mechanisms in Maize. *Mol. Plant.* **10,** 389-401.